MODELLING GEOMETRY INTERRUPTION, VASCULAR STRESS, AND PULSATILITY IN CAROTID ARTERY BLOOD FLOW USING POISEUILLE-BASED EQUATIONS

LUCY JEROP NGETICH

A THESIS SUBMITTED TO THE SCHOOL OF SCIENCE IN PARTIAL FULFILLMENT FOR THE DEGREE OF MASTER OF SCIENCE IN APPLIED MATHEMATICS, OF THE UNIVERSITY OF ELDORET, KENYA

2025

DECLARATION

Declaration by the Student

This work is my original work and has not been submitted for a degree award in any other University, and shall not be reproduced in part or full, or in any format without prior written permission from the author and/or University of Eldoret.

Signature:.....Date:.....

LUCY JEROP NGETICH

SSCI/MAT/M/002/20

Declaration by the Supervisors

This thesis has been submitted for examination with our approval as the University Supervisors

DR. MAREMWA SHICHIKHA

Department of Mathematics and Computer Science

University of Eldoret, Kenya

Signature:.....Date:.....

DR. KANDIE JOSEPH

Department of Mathematics and Computer Science

University of Eldoret, Kenya

Signature:.....Date:.....

DEDICATION

I dedicate this thesis to my dear husband, Barnabas Boit and my lovely children Lewis and Emma.

ACKNOWLEDGEMENTS

I want to express my gratitude to my supervisors for their guidance and support throughout the development of this research project.

ABSTRACT

The Poiseuille equations are instrumental in modeling blood flow, particularly within large and medium-sized arteries where laminar flow predominates. Derived under the assumption of steady, incompressible, Newtonian flow through cylindrical tubes, these equations effectively describe vascular dynamics in geometries approximating cylindrical shapes and at low Reynolds numbers. However, their applicability diminishes in regions characterized by turbulence, geometric irregularities, or pulsatile flow, such as those found in the carotid artery. This study identifies three key research gaps in the application of Poiseuille equations to carotid artery hemodynamics: (i) the influence of vascular shear stress under turbulent conditions, (ii) the deviation introduced by pulsatile flow from the steady-state assumption inherent in the Poiseuille model, and (iii) the geometric variability of the carotid artery and its underexplored role in altering flow characteristics. To address these gaps, the study introduces a novel formulation of the Poiseuille equation incorporating geometric drag and pulsatile flow through a Womersley function. Governing equations were formulated based on modified Poiseuille flow and solved numerically using the Finite Volume Method (FVM) implemented in MATLAB, with custom code developed to simulate time-dependent blood flow. The numerical scheme incorporated discretization of the Navier–Stokes equations and was executed using MATLAB's built-in solvers and post-processing tools for velocity, pressure, and vascular stress visualization. The simulation results revealed a significant reduction in flow rate and velocity in regions with geometric interruptions. For example, the peak simulated velocity reduced by approximately 28% in stenosed segments compared to normal arterial sections, demonstrating a nonlinear velocity profile consistent with observed clinical behavior. The simulations further indicated that geometric disturbances, such as stenosis and bifurcations, resulted in an increase in vascular stress and a pronounced decrease in flow rate (Q), particularly under turbulent conditions. This inverse relationship between vessel radius and flow dynamics corroborates findings from existing studies on stenotic arteries. Additionally, the analysis demonstrated that as artery radius (r) decreased, vascular stress $W(r,t)$ increased substantially, in line with predictions from Hagen–Poiseuille's law. Pulsatility during systolic phases further amplified wall shear stress (WSS), thus supporting the third objective of the study. The findings emphasize the limitations of the classical Poiseuille-based model in turbulent and pulsatile regimes and highlight the necessity for more robust modeling approaches to accurately capture the complex hemodynamics of carotid artery flow under pathological conditions.

TABLE OF CONTENTS

LIST OF TABLES

LIST OF FIGURES

LIST OF NOTATION AND ABBREVIATIONS

Symbol/Abbreviation	Description	Unit
Q	Flow rate	$\mathrm{m^3\,s^{-1}}$
r	Radius of the artery	m
P	Pressure difference	Pa
ΔP	Pressure drop	Pa
f	Drag coefficient	dimensionless
L	Length of the artery	m
ρ	Density of blood	$\mathrm{kg\,m^{-3}}$
V	Velocity of blood	$\mathrm{m\,s^{-1}}$
μ	Viscosity of blood	$\mathrm{Pa\,s}$
D_c	Carotid diameter	m
P_r	Heart rate	$\mathrm{min^{-1}}$
$ECCO_2R$	Extracorporeal Carbon Dioxide Removal	–
ANSYS	Analysis System	
BBB	Blood-Brain Barrier	
CBF	Cerebral Blood Flow	
CFD	Computational Fluid Dynamics	
CNS	Central Nervous System	
CT	Computed Tomography	
ECMO	Extracorporeal Membrane Oxygenation	
FVM	Finite Volume Method	
HAWB	Horner-Armstrong-Wagner-Beris	
RBC	Red Blood Cell	
Re	Reynolds Number	dimensionless
VA	Venoarterial	
VAD	Ventricular Assist Devices	
VV	Venovenous	
VVA	Venovenoarterial	

CHAPTER ONE

INTRODUCTION

1.1 Background Information

Blood flow in arteries is a complex phenomenon influenced by various factors, including the rheological properties of blood, the geometric characteristics of arteries, and the dynamic behavior of the circulatory system (Dutra et al., 2021; Kannojiya et al., 2020; Wajihah and Sankar, 2023). Mathematical modeling of blood flow has traditionally relied on Navier-Stokes equations (Avgerinos and Neofytou, 2019; Liu et al., 2021). While these equations have been valuable in stimulating blood flow, the Poiseuille equations have the potential to provide a more straightforward yet more insightful representation of arterial blood flow. The Poiseuille equations, derived from the principles of fluid dynamics, describe laminar flow in cylindrical tubes, which align well with the structure of arteries.

The Poiseuille equations are applicable in modeling blood flow under certain conditions due to their relevance in describing laminar flow in cylindrical tubes (Nichols, 2022). The applicability of Poiseuille equations in modeling blood flow is attributed to many factors, including laminar flow assumptions, tube geometry, and pulsatility. The Poiseuille equations are derived based on the assumption of laminar flow, which means that the fluid moves in smooth, parallel layers with minimal turbulence. Blood flow in large and medium-sized arteries and arterioles often exhibits laminar characteristics, particularly when the Reynolds number is below a critical value (Lopes et al., 2020). In these conditions, the Poiseuille equations provide a reasonably accurate representation of blood flow. The Poiseuille equations were originally developed to describe flow in cylindrical tubes (Pisano and Pisano, 2021). Many blood ves-

sels, especially arteries, have approximately cylindrical shapes over significant portions of their length. This makes the Poiseuille equations suitable for modelling blood flow in these vessels. Blood is nearly incompressible under physiological conditions. The Poiseuille equations assume incompressible flow, which aligns with the behaviour of blood in the circulatory system (Blokhin and Tkachev, 2020). The Poiseuille equations apply to Newtonian fluids, which include blood within the typical range of shear rates found in arteries. Blood viscosity, although non-constant, can be considered approximately constant for most modelling purposes. The Poiseuille equations are often applied under steady-state or quasi-steady flow conditions. This simplification is suitable for many modelling scenarios, especially when analyzing long-term trends in blood flow. The Reynolds number (Re) is often relatively low in arteries and arterioles due to the small diameters and low flow rates. Low Re values indicate that the flow is more likely to be laminar, further justifying using the Poiseuille equations. However, Poiseuille equations have limitations and may not be applicable in all situations. For instance, in smaller blood vessels such as capillaries and regions of disturbed or turbulent flow, the assumptions of the Poiseuille equations break down (Ashoor et al., 2021). In small vessels like blood capillaries, blood flow is often disturbed or turbulent, and the assumptions and simplifications underlying the Poiseuille equations break down. In such situations, more complex equations, such as the Navier-Stokes equations, are necessary to model the flow behaviour accurately. Thus, in the proposed research, the study will be limited to blood flow in the Carotid artery for a case of a uniform reduction of the carotid artery. The carotid artery supplies blood to the head and neck, often exhibiting laminar flow. These arteries are relatively large and have smooth, straight sections that promote laminar flow.

A uniform reduction in the diameter of blood arteries, known as arterial stenosis (Abnormal narrowing of a bodily canal or passageway) or constriction, can introduce disturbances in blood flow (Dhange et al., 2022a). This reduction in diameter can result from atherosclerosis (A stage of arteriosclerosis involving fatty deposits (atheromas) inside the arterial walls, thus narrowing the arteries), arterial plaque buildup, or other pathological conditions. The

disturbances in blood flow caused by arterial stenosis can lead to various hemodynamic effects and clinical implications, including turbulence and changes in blood pressure. As the cross-sectional area of the artery decreases due to stenosis, the blood velocity must increase to maintain the same volumetric flow rate (according to the principle of continuity). This increase in velocity can result in higher shear stress on the arterial walls and, in some cases, transition the flow from laminar to turbulent. The flow may become turbulent in arteries with severe stenosis, characterized by chaotic, irregular flow patterns (Freidoonimehr et al., 2020). Turbulence can lead to increased friction and energy losses and may damage the endothelial lining of the artery. Turbulent flow is associated with a higher risk of thrombosis and emboli formation. Stenotic regions can create low-pressure zones immediately downstream, which can contribute to the development of blood clots or thrombosis. Low-pressure zones can also reduce the flow of oxygenated blood to downstream tissues. Disturbances in flow patterns, such as recirculation zones and vortices, can develop around the stenotic region (Owais et al., 2023). These disturbances can alter the distribution of blood cells, affecting the oxygen supply to tissues and potentially contributing to the development of atherosclerotic plaques. Hemodynamic changes caused by stenosis can lead to wall shear stress variations along the artery. This can affect endothelial cells' function and lead to endothelial dysfunction, inflammation, and increased risk of atherosclerosis development. In areas of disturbed flow, platelets and other blood components may be more likely to aggregate, increasing the risk of embolism or clot formation. These emboli can then travel to smaller arteries and obstruct blood flow, potentially leading to serious complications.

1.2 Basic Concepts

1.2.1 Fundamentals of Blood Flow Dynamics

Blood, a complex fluid comprising red and white blood cells, platelets, and plasma, exhibits different flow characteristics depending on vessel size (Kannojiya et al., 2020). In smaller vessels, blood behaves as a non-Newtonian fluid, with its viscosity varying with shear rate

(Wajihah and Sankar, 2023). However, in large arteries such as the aorta, blood is often approximated as a Newtonian fluid, where viscosity remains constant, simplifying the analysis. The theoretical modeling of blood flow is governed by fundamental fluid dynamics principles. The two primary equations used are the continuity equation, which ensures mass conservation, and the Navier-Stokes equations, which describe the conservation of momentum. This section focuses on the continuity equation and its role in blood flow modeling.

1.2.1.1 Continuity Equation

The continuity equation describes the principle of mass conservation in fluid dynamics. For blood, which can be treated as an incompressible fluid in large vessels, the general form of the continuity equation is (Kumar et al., 2022; Moreles et al., 2013):

$$\frac{\partial \rho}{\partial t} + \nabla \cdot (\rho \mathbf{u}) = 0 \tag{1.1}$$

where ρ is the density of blood, $\mathbf{u}$ is the velocity field of the blood flow, t is time. This equation states that the rate of change of density within a given volume plus the net flux of mass across the boundary of that volume must equal zero.

1.2.1.2 Simplification for Incompressible Fluids

In the case of incompressible fluids, where the density ρ is constant, the equation simplifies significantly. Since $\frac{\partial \rho}{\partial t} = 0$, the continuity equation reduces to (Farkhutdinov et al., 2020):

$$\nabla \cdot \mathbf{u} = 0 \tag{1.2}$$

This simplified form implies that the velocity field is divergence-free, meaning there is no net change in the volume of the fluid element. In essence, for every infinitesimal volume of blood, the amount entering must equal the amount leaving (Spencer, 2020). This ensures that the mass of blood is conserved throughout the flow.

1.2.2 Physiological Interpretation

The incompressible assumption holds true for blood in large vessels, such as arteries, where the change in density is negligible (Myneni and Rajagopal, 2022). The continuity equation plays a crucial role in describing the movement of blood through the circulatory system. For instance, in an artery, the velocity of blood adjusts based on changes in the vessel's cross-sectional area to maintain constant mass flow. When a vessel narrows, the velocity increases; when it widens, the velocity decreases.

1.2.2.1 Application to Vessel Networks

In branching networks of blood vessels, the continuity equation ensures that the total amount of blood entering a junction equals the total amount leaving it (Ghitti et al., 2022). This is essential in computational simulations of the cardiovascular system, where maintaining the mass balance is crucial for accurate modeling of blood distribution. The equation helps predict how blood flows through complex vascular networks, accounting for changes in velocity due to vessel diameter and bifurcation.

1.2.2.2 Blood Flow in a Vessel

Consider blood flowing through a cylindrical vessel with a varying diameter. The continuity equation ensures that the mass of blood remains constant as it flows through different sections of the vessel (Bertaglia et al., 2020). Since blood is treated as an incompressible fluid in large arteries, the volumetric flow rate must remain constant at all points along the vessel. This relationship is given by:

$$A_1 u_1 = A_2 u_2 \tag{1.3}$$

where A_1 and A_2 are the cross-sectional areas of the vessel at two different points, u_1 and u_2 are the corresponding blood velocities. Equation (1.3) represents the conservation of mass for incompressible fluids. It implies that the product of the cross-sectional area and velocity

remains constant along the length of the vessel. If the diameter of the vessel changes, the velocity must adjust accordingly to maintain a constant flow rate. For instance, if the vessel narrows at a point such that $A_2 < A_1$, the velocity at that point must increase ($u_2 > u_1$). This is because a decrease in cross-sectional area necessitates an increase in velocity to ensure the same volume of blood passes through per unit time. Conversely, if the vessel widens ($A_2 > A_1$), the velocity decreases ($u_2 < u_1$). This principle is crucial in understanding blood flow dynamics in the human body, particularly in large arteries like the aorta, where blood flow velocities and vessel diameters vary. The relationship between area and velocity helps explain how blood adapts to changes in vessel geometry to maintain efficient circulation throughout the body (Alexy et al., 2022).

1.2.2.3 Navier-Stokes Equations for Blood Flow

Blood, although a complex fluid with both solid and liquid components, can be modeled as an incompressible, Newtonian fluid when studying flow in large arteries (Wajihah and Sankar, 2023). For an incompressible, Newtonian fluid, the Navier-Stokes equations are expressed as:

$$\rho\left(\frac{\partial \mathbf{u}}{\partial t} + \mathbf{u}\cdot\nabla\mathbf{u}\right) = -\nabla p + \mu\nabla^2\mathbf{u} + \mathbf{f} \tag{1.4}$$

where ρ is the fluid density (in this case, blood), $\mathbf{u}$ is the velocity vector field, p is the pressure field, μ is the dynamic viscosity of the fluid, ∇^2 is the Laplacian operator, representing the second spatial derivatives, $\mathbf{f}$ is the external force field acting on the fluid.

Each term in the Navier-Stokes equations plays a significant role in describing the forces acting on the fluid and how they influence its motion:

- The term $\frac{\partial \mathbf{u}}{\partial t}$ represents the local acceleration, or the rate of change of velocity with respect to time at a specific point in the fluid.
- The term $\mathbf{u}\cdot\nabla\mathbf{u}$ is the convective acceleration, a nonlinear term that accounts for

changes in velocity as fluid particles move through the velocity field. This term introduces the complexity of fluid motion, as it captures the interactions between different fluid layers and their respective velocities.

- The pressure gradient term, ∇p, drives the fluid flow. Blood moves from regions of higher pressure to lower pressure, and this term accounts for the force exerted by the pressure difference within the fluid.

- The viscous term, $\mu\nabla^2\mathbf{u}$, represents viscous diffusion. This term models how internal friction within the fluid (due to its viscosity) resists changes in velocity. The Laplacian operator, ∇^2, captures the spatial variation of the velocity field, and μ controls the rate at which momentum is diffused through the fluid due to viscous effects.

- Finally, $\mathbf{f}$ accounts for external forces acting on the fluid, such as gravitational forces or forces due to the surrounding tissue in the case of blood flow.

For blood flow in large arteries, the Navier-Stokes equations help describe how momentum is conserved while taking into account forces like pressure and viscosity (Siddqi, 2024). Blood flow is primarily driven by the heart's pumping action, which generates pressure differences throughout the circulatory system. The pressure gradient term, ∇p, models this driving force, while the viscous term, $\mu\nabla^2\mathbf{u}$, ensures that the viscosity of blood, caused by the interactions between blood cells and plasma—slows down the fluid in regions where velocity gradients exist. In large arteries, such as the aorta, blood can be approximated as a Newtonian fluid because the shear rates are high, and the effect of blood's non-Newtonian properties is minimized. The assumption of incompressibility simplifies the analysis, as it implies that the density of blood remains constant, meaning that the continuity equation applies, as discussed earlier.

One of the most challenging aspects of the Navier-Stokes equations is the nonlinear convective term, $\mathbf{u}\cdot\nabla\mathbf{u}$ (Kollmann, 2024). This term arises due to the nature of fluid flow, where the velocity of a fluid particle changes as it moves through different regions of the velocity field.

The nonlinearity of this term makes solving the Navier-Stokes equations analytically difficult in most practical cases, necessitating numerical methods and computational simulations for complex blood flow scenarios.

1.2.3 Non-Newtonian Nature of Blood

Blood, although often approximated as a Newtonian fluid in large vessels, exhibits non-Newtonian behavior, particularly in smaller vessels and under low shear conditions. This non-Newtonian nature arises due to the complex composition of blood, which is a suspension of various cellular components such as red blood cells (RBCs), white blood cells, and platelets, all suspended in plasma. The interactions between these components and their response to varying shear rates lead to changes in blood's viscosity, making it dependent on the flow conditions (Wang et al., 2022). In smaller vessels, such as arterioles, capillaries, and venules, where the diameter is small and the shear rates are low, the behavior of blood becomes distinctly non-Newtonian. This variation in behavior must be captured using more sophisticated models than the simple Newtonian approximation. One of the most commonly used models to describe blood's non-Newtonian behavior is the Casson model, which relates shear stress to the shear rate in a nonlinear fashion (Shahzad et al., 2022).

1.2.3.1 The Casson Model

The Casson model describes the shear-thinning behavior of blood. Shear-thinning fluids exhibit a decrease in viscosity with increasing shear rate, which is characteristic of blood under physiological conditions. The model is given by the following equation:

$$\tau^{1/2} = \tau_0^{1/2} + \eta^{1/2}\dot{\gamma}^{1/2} \tag{1.5}$$

where τ is the shear stress, τ_0 is the yield stress, which represents the minimum stress required for the fluid to start flowing, η is the plastic viscosity, representing the inherent resistance of the fluid to flow, $\dot{\gamma}$ is the shear rate, which measures the rate at which adjacent layers of fluid

move relative to each other.

The model in Equation (1.5) is particularly useful for capturing blood flow behavior at low shear rates, where the non-Newtonian effects are most pronounced. At high shear rates, such as those found in large arteries, blood's behavior approaches that of a Newtonian fluid, where viscosity becomes nearly constant and independent of the shear rate (Carvalho et al., 2021). However, in small vessels or under slow flow conditions, yield stress τ_0 plays a critical role. Blood must overcome this yield stress before it begins to flow, a key factor in understanding blood behavior in microcirculation.

The Casson model has significant physiological implications, particularly in microcirculation (Roy and Bég, 2021). In small vessels like capillaries, blood behaves as a viscoplastic fluid. When the shear rate is low, such as in venules or during periods of low blood flow, the yield stress τ_0 prevents blood from flowing freely. This leads to phenomena such as the Fahraeus-Lindqvist effect, where the apparent viscosity of blood decreases as the vessel diameter decreases, allowing for more efficient blood flow in narrow vessels. However, at higher shear rates such as in exercise or larger arteries, viscous blood flows over the yield stress more readily and the viscosity is reduced. This shear-thinning behavior allows blood to easily flow through large and small vessels, adapting to the various needs that the body requires for oxygen and nutrients.

Although the Casson model is properly able to describe the shear thinning transition of blood, it has some drawbacks (Kannojiya, 2020, Simulation of physiological system). The model assumes an easily calculable relationship between shear stress and shear rate that, in reality, does not necessarily resemble the nature of the interactions of blood cellular components. More complex models, like the Carreau-Yasuda model, can better describe the non-Newtonian behavior of blood over a broader range of shear rates and flow conditions. Nevertheless, the Casson model is still very commonly used to comprehend blood rheology in less large vessels and under low shear stress where its predictive performance is very high.

1.2.4 Boundary Conditions

The solution of the Navier-Stokes equations and the continuity equation is essential for modeling fluid flow within different physical systems, including blood flow in vessels. However, these equations cannot be solved without specifying appropriate boundary conditions, which are critical to ensuring the model reflects the physical reality of the problem. Boundary conditions help define the interaction between the fluid and its surroundings, influencing the velocity, pressure, and other flow properties within the computational domain.

Boundary conditions are a vital component when solving the Navier-Stokes and continuity equations, as they provide the necessary constraints for determining a unique solution (Gazzola and Sperone, 2020). In practical applications, such as fluid flow in artery, channels, or biological systems like blood vessels, these conditions define how the fluid interacts with the boundaries of the domain, including walls, inlets, and outlets. The choice of boundary conditions depends on the physical characteristics of the flow and the computational model being used. The most common boundary conditions used in fluid flow problems:

- **No-slip condition**: One of the most widely applied boundary conditions is the no-slip condition, which assumes that at a solid boundary (such as the wall of a artery or vessel), the fluid's velocity is equal to that of the boundary itself (Rougier et al., 2021). For a stationary wall, this means that the velocity of the fluid at the wall is zero. This condition reflects the physical reality that viscous fluids adhere to solid surfaces due to molecular interactions and is described by (1.6):

$$\mathbf{u} = 0 \quad \text{on the vessel wall} \tag{1.6}$$

  The no-slip condition is crucial when modeling viscous flows, as it ensures that the fluid's velocity diminishes to zero at solid boundaries, allowing for the accurate prediction of flow behavior near walls, such as the development of boundary layers and shear stresses (Wedel et al., 2022).

- **Inlet and outlet conditions**: Inlet and outlet boundary conditions specify the behavior of the fluid as it enters and leaves the computational domain (Holmes and Pivonka, 2021). These conditions are necessary to drive the flow through the system and ensure that the simulation accurately represents the physical system. At the inlet, one common approach is to prescribe a velocity profile, which could be uniform, parabolic, or based on experimental data. Alternatively, a flow rate might be specified, which can then be converted into a velocity profile using the continuity equation. In cases where experimental or empirical data is available, the velocity profile might be adjusted to better match the actual conditions observed in practice. A prescribed velocity profile at the inlet could take the following form described by Equation (1.7)

$$\mathbf{u}(x_0, y, z) = f(y, z) \tag{1.7}$$

where $f(y, z)$ represents the functional form of the velocity distribution in the cross-section of the vessel. At the outlet, the boundary condition typically involves specifying either a pressure value or a stress-free condition. The pressure-based outlet condition assumes that the fluid exits the domain at a known pressure, often set to atmospheric pressure for open systems. The stress-free outlet condition, on the other hand, assumes that the normal and tangential stresses vanish at the boundary, which is appropriate for scenarios where the flow is relatively unimpeded at the exit.

For an outlet with a specified pressure condition, the boundary condition might be written as:

$$p = p_{\text{out}} \quad \text{at the outlet} \tag{1.8}$$

where p_{out} is the known outlet pressure. Alternatively, for a stress-free outlet, the condition might take the form:

$$\mathbf{n} \cdot \sigma = 0 \quad \text{at the outlet} \tag{1.9}$$

where $\mathbf{n}$ is the unit normal vector to the outlet surface, and σ is the stress tensor.

Boundary conditions play a critical role in ensuring the stability and accuracy of numerical simulations of fluid flow. When improperly chosen, they can lead to non-physical results, such as unrealistic velocity distributions or spurious pressure gradients (Mimeau and Mortazavi, 2021). Therefore, selecting appropriate boundary conditions that accurately reflect the physical properties and constraints of the system is essential for obtaining reliable and meaningful results from the simulation. In many practical applications, particularly in the field of biomedical engineering, boundary conditions may need to be derived from experimental data. For example, when modeling blood flow through arteries, the inlet velocity profile might be obtained from Doppler ultrasound measurements, while the outlet pressure condition might be based on clinical data on arterial blood pressure. In such cases, the boundary conditions not only define the interaction between the fluid and its surroundings but also serve as an important link between the computational model and real-world observations.

In addition to the standard boundary conditions described above, more specialized conditions may be required for complex or multi-phase flows. For instance, in cases where fluid interacts with a porous medium or a moving boundary (such as a deformable blood vessel wall), additional conditions might be needed to account for the exchange of momentum and mass across the boundary. Another aspect to consider is the choice of boundary conditions for turbulent flow. While the no-slip condition still applies at solid walls, turbulence models may require additional boundary conditions to define the behavior of turbulent quantities, such as turbulence intensity or eddy viscosity, at the boundaries. These conditions are crucial for accurately capturing the effects of turbulence on the flow, especially in high Reynolds number flows where turbulence plays a dominant role in the overall flow behavior.

1.2.5 Simplified Models of Blood Flow

1.2.5.1 Poiseuille Flow

The blood flow within long, straight vessels under steady-state conditions can be simplified using a model known as Poiseuille's law (Saktioto et al., 2023). This law provides an analytical solution for the volumetric flow rate in a cylindrical vessel, assuming certain idealized conditions such as fully developed, laminar flow. This equation plays an important role in understanding the behavior of blood flow, especially in smaller vessels like capillaries and arterioles, where assumptions of laminar flow are often valid. The equation is expressed as:

$$Q = \frac{\pi R^4 \Delta P}{8 \mu L} \tag{1.10}$$

where Q represents the volumetric flow rate (the volume of fluid flowing through the vessel per unit of time), R is the radius of the vessel, ΔP is the pressure drop across the length L of the vessel, μ is the dynamic viscosity of the fluid (blood in this case), L is the length of the vessel. Equation (1.10) is derived from the Navier-Stokes equations under the assumptions of steady-state, incompressible, and Newtonian fluid behavior in a cylindrical artery or vessel. It provides a simplified model that is particularly useful for analyzing blood flow in small vessels where the assumptions of Poiseuille's law reasonably hold. Poiseuille's law is derived by solving the Navier-Stokes equation for an incompressible, Newtonian fluid in a cylindrical artery under the following conditions (Yadav et al., 2020):

- **Steady-state flow**: The flow does not change over time.
- **Laminar flow**: The flow is smooth and orderly, with fluid layers sliding past one another without mixing. Laminar flow occurs when the Reynolds number, a dimensionless quantity that compares inertial forces to viscous forces, is low. In blood vessels, this typically corresponds to smaller diameters and lower flow velocities.
- **Fully developed flow**: The velocity profile of the fluid remains consistent along the

length of the vessel. This assumption means that the parabolic velocity profile has reached equilibrium, with a maximum velocity at the center of the vessel and zero velocity at the vessel walls (no-slip condition).

- **Newtonian fluid**: Poiseuille's law assumes the fluid has a constant viscosity. While blood is technically a non-Newtonian fluid because its viscosity varies with shear rate, the approximation of constant viscosity is reasonable in many cases for small vessels and moderate flow rates.

- **Rigid cylindrical vessel**: The vessel walls are assumed to be rigid and cylindrical in shape. In reality, biological vessels, such as arteries and veins, are elastic, and their diameter can change due to pressure. However, for small vessels or under conditions where deformations are small, this assumption can still provide useful insights.

Under these assumptions, the velocity profile $u(r)$ in a artery is parabolic, and the volumetric flow rate Q is proportional to the pressure gradient $\Delta P/L$, the radius of the vessel raised to the fourth power, and inversely proportional to the dynamic viscosity μ and the length of the vessel L.

$$u(r) = \frac{\Delta P}{4\mu L}(r^2 - R^2) \tag{1.11}$$

where r is the radial distance from the center of the vessel, and $u(r)$ represents the fluid velocity at that point. The velocity is maximum at the center of the vessel ($R = 0$) and zero at the vessel wall ($r = R$) due to the no-slip condition. Integrating this velocity profile over the cross-sectional area of the vessel gives Poiseuille's law for the volumetric flow rate.

Poiseuille flow parameters are significance. For instance, Vessel Radius R, which is one of the most important features of Poiseuille's law is its dependence on the radius of the vessel raised to the fourth power (Nichols, 2022). This means that even small changes in the vessel radius have a dramatic impact on the flow rate. For example, if the radius of a blood vessel doubles, the flow rate increases by a factor of 16. This sensitivity to radius is critical in under-

standing how physiological processes, such as vasoconstriction (narrowing of blood vessels) or vasodilation (widening of blood vessels), regulate blood flow. In the human circulatory system, arteries and arterioles can change their diameter through the contraction or relaxation of smooth muscle in their walls, allowing the body to control blood flow to different organs or tissues (Kim, 2022). Poiseuille's law helps explain how even small adjustments to vessel diameter can have significant effects on blood circulation.

The pressure drop ΔP across the vessel drives the flow of blood (Campinho et al., 2020). It is the difference in pressure between the inlet and the outlet of the vessel. Blood pressure is generated primarily by the heart's pumping action, with the highest pressure found near the heart and progressively lower pressures as blood moves through the systemic circulation. In Poiseuille's law, the greater the pressure drop, the higher the volumetric flow rate. However, the pressure drop is also influenced by the resistance to flow within the vessel, which depends on factors like vessel length, viscosity, and, most importantly, vessel radius. In the systemic circulation, arterioles act as the primary resistance vessels, creating significant pressure drops and controlling the flow of blood to various tissues.

The dynamic viscosity μ represents the fluid's resistance to deformation (Li et al., 2021). In blood flow, viscosity depends on factors like hematocrit (the proportion of red blood cells in the blood) and shear rate (Trejo-Soto and Hernández-Machado, 2022). While blood is a non-Newtonian fluid, Poiseuille's law assumes constant viscosity, providing a useful approximation for certain flow conditions, especially in small vessels where shear rates are relatively low. Higher blood viscosity leads to greater resistance to flow and, consequently, a lower flow rate for a given pressure drop. In conditions where blood viscosity increases, such as in polycythemia (an abnormally high red blood cell count), Poiseuille's law helps explain why higher pressures are needed to maintain adequate blood flow.

The vessel length L is inversely proportional to the flow rate. Longer vessels result in greater frictional resistance to flow, reducing the volumetric flow rate for a given pressure drop (Gamal et al., 2021). This is one reason why the circulatory system uses many short,

branching vessels rather than a few long ones, shorter vessels minimize resistance and make the distribution of blood more efficient.

While Poiseuille's law provides valuable insights into blood flow in small vessels, it has several limitations. It applies strictly to laminar, steady-state flow in rigid, cylindrical vessels (Chen et al., 2023). In larger vessels, where flow can become turbulent, or in situations where the vessel walls are elastic and undergo significant deformation, more complex models are required. Additionally, the assumption of constant viscosity is not always accurate for blood, particularly in capillaries where blood exhibits non-Newtonian behavior.

1.2.5.2 Womersley Flow

In large arteries where pulsatile flow occurs due to the heart's rhythmic pumping, Womersley's theory is applicable. The Womersley number, a dimensionless parameter, characterizes this flow:

$$\alpha = R \left(\frac{\omega \rho}{\mu} \right)^{1/2} \tag{1.12}$$

where ω is the angular frequency of the heart rate. For large Womersley numbers, the flow exhibits significant pulsatility and non-parabolic velocity profiles.

1.2.6 Numerical Methods for Solving Blood Flow Equations

Given the complexity of solving the Navier-Stokes equations analytically, numerical methods such as the Finite Element Method (FEM) and Finite Volume Method (FVM) are widely used.

1.2.6.1 Finite Element Method (FEM)

FEM discretizes the computational domain into small elements and applies the weak form of the governing equations. For the Navier-Stokes equations, the weak form is given by:

$$\int_\Omega \rho \left(\frac{\partial \mathbf{u}}{\partial t} + \mathbf{u} \cdot \nabla \mathbf{u} \right) \cdot \mathbf{v} \, d\Omega + \int_\Omega \mu \nabla \mathbf{u} : \nabla \mathbf{v} \, d\Omega = \int_\Omega p \nabla \cdot \mathbf{v} \, d\Omega \tag{1.13}$$

where $\mathbf{v}$ is a test function and Ω is the computational domain.

1.2.6.2 Finite Volume Method (FVM)

FVM integrates the governing equations over control volumes and ensures conservation laws are satisfied within each volume. This method is particularly useful in complex geometries and for fluid dynamics problems, including blood flow.

1.2.7 Carotid Blood Flow

Modeling carotid blood flow using the Poiseuille equation involves concepts related to fluid dynamics and the circulatory system. The Poiseuille equation is used to describe the relationship between blood flow, pressure, and the characteristics of the blood vessels, particularly in this case, the carotid artery (See Figure 1.1). Carotid blood flow is the volume of blood that flows through the carotid artery per unit time. It can be measured non-invasively using a flow meter that allows simultaneous measurement of artery diameters by a mode ultrasound and velocity measurements by an angle-insensitive method (Skytioti et al., 2019). It can also be calculated as:

$$C_f = \pi \times \frac{D_C^2}{4} \times \int_{t_0}^{t_i} v dt p_r \tag{1.14}$$

where C_f is Carotid blood flow, D_c is carotid diameter, $\int_{t_0}^{t_i} v$ is velocity time integral and p_r is heart rate.

1.2.8 Poiseuille Equation

The Poiseuille equation is a fundamental equation in fluid dynamics used to calculate blood flow through a cylindrical vessel like an artery (Nichols, 2022). It is derived from the principles of fluid dynamics and describes how blood flow (Q) is related to the pressure difference (ΔP), the radius $(D_c/2)$ of the vessel, the length (L) of the vessel, and the viscosity (μ) of

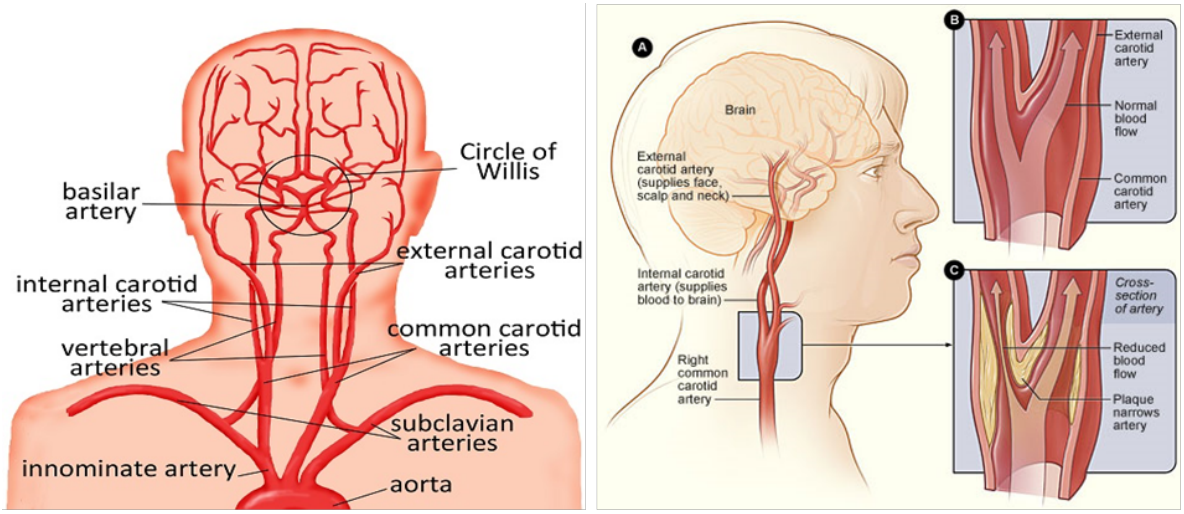

Figure 1.1: Carotid Arteries
Source: (Heck and Jost, 2021)

the blood. The equation is as follows:

$$Q = \frac{\pi \Delta P r^4}{8 \mu L} \tag{1.15}$$

Pressure Difference (ΔP) represents the pressure gradient between two points along the carotid artery. This pressure gradient is the driving force behind blood flow. The difference in pressure is what causes blood to move from areas of higher pressure to lower pressure. Vessel Radius r is the radius of the carotid artery which plays a crucial role in determining blood flow. The Poiseuille equation demonstrates that the flow is directly proportional to the fourth power of the vessel radius. This means that even small changes in the radius of the artery can significantly affect blood flow. Viscosity (μ) refers to the thickness or resistance of a fluid to flow. Factors like hematocrit and temperature influence blood viscosity, and are inversely proportional to blood flow. Higher viscosity results in decreased blood flow. Length (L) is the length of the carotid artery. Longer arteries offer more resistance to blood flow, which can affect the overall flow rate.

1.2.9 Womersley function

The Womersley function is named after British engineer and mathematician John Womersley, who significantly contributed to the study of pulsatile flow in biological systems (Womersley, 1955). Womersley function is often denoted as $W(r,t)$, describes the temporal variation of velocity profiles in a pulsatile flow regime, such as the flow of blood through arteries like the carotid artery. It considers the effects of both convection (advection) and diffusion (viscosity) in the flow. The Womersley function captures pulsatile nature of blood flow associated with rhythmic contraction of the heart. It also describes how the velocity of blood changes over time and along the cross section of the artery. When used with Poiseuille equation in the case of blood flow, the modified equation becomes time-dependent and provides a more accurate representation of blood flow in arteries under dynamic conditions. It is influenced by boundary conditions at the inlet and outlet of the artery, including pressure waveforms and flow rate profiles and offers a more realistic representation of blood flow in biological systems.

1.2.10 The governing equations

Unlike existing studies, the research considers the blood flow in the Carotid artery during accidents. During accidents, the Carotid artery experiences vascular stress with varied pulse flow and shifted geometry, which complicates the blood flow. The internal diameter of the carotid arteries varies with sex, and age. The decrease in carotid artery diameter resulting in decreased carotid artery blood flow occurs within three minutes of injury, which is consistent with the timing of injury (Clevenger et al., 2015). Carotid arterial diameter enlargement is a manifestation of arterial remodelling (See Figure 1.2) and may be a risk factor for cardiovascular disease, which often leads to 40% deaths (Sedaghat et al., 2018). Carotid artery aneurysms (A cardiovascular disease characterized by a saclike widening of an artery resulting from weakening of the artery wall) may develop after a serious car accident, which can cause internal bleeding and prevent blood from flowing to the brain, leading to brain damage (Babich, 2021). The research considers two aspects of the carotid artery during accidents: the

existence of reduced diameter and the swollen section. The proposed governing equation is composed of three aspects bridging the gap existing in the literature. From Equation (1.15), that is, the drag force function due to shear stress due to accidents in the carotid artery is introduced.

$$Q = \frac{\pi}{8\mu L}\left(r^4\right)\left(P - \Delta P - f\left(\frac{L}{2r}\right)\left(\frac{\rho V^2}{2}\right)\right) \tag{1.16}$$

where Q is the flow rate, r is the radius of the artery, P is the pressure difference between the two ends of the artery, ΔP is the pressure drop due to the reduced arterial diameter, f is the drag coefficient, L is the length of the artery, ρ is the density of blood, V is the velocity of blood, μ is the viscosity of blood and is summarized in Table 1.1. The drag coefficient f is given by

$$\begin{aligned} f &= \tfrac{64}{Re} \\ R_e &= \tfrac{2\rho V r}{\mu} \end{aligned} \tag{1.17}$$

Table 1.1: Parameter description

Parameter	Description
Q	flow rate
r	radius of the artery
P	pressure difference between the two ends of the artery
ΔP	pressure drop due to the reduced arterial diameter
f	drag coefficient
L	length of the artery
ρ	density of blood
V	velocity of blood
μ	viscosity of blood.

Thus, Equation (1.17) can be written as

$$\begin{aligned} Q = &\ \tfrac{\pi}{8\mu L}\left(r^4\right)\left(P - \Delta P - \left(\tfrac{64\mu}{2\rho V r}\right)\left(\tfrac{L}{2r}\right)\left(\tfrac{\rho V^2}{2}\right)\right) \\ = &\ \tfrac{\pi}{8\mu L}\left(r^4\right)\left(P - \Delta P - \tfrac{8\mu L V}{r^2}\right) \end{aligned} \tag{1.18}$$

Introducing the Womersley function to include the temporal variation of velocity profiles in

a pulsatile flow due to accidents and changes in artery diameter. Equation (1.17) becomes

$$Q = \frac{\pi}{8\mu L}\left(r^4\right)\left(P - \Delta P - \frac{8\mu L V}{r^2}\right) + W(r,t) \tag{1.19}$$

where $W(r,t)$ is the Womersley function

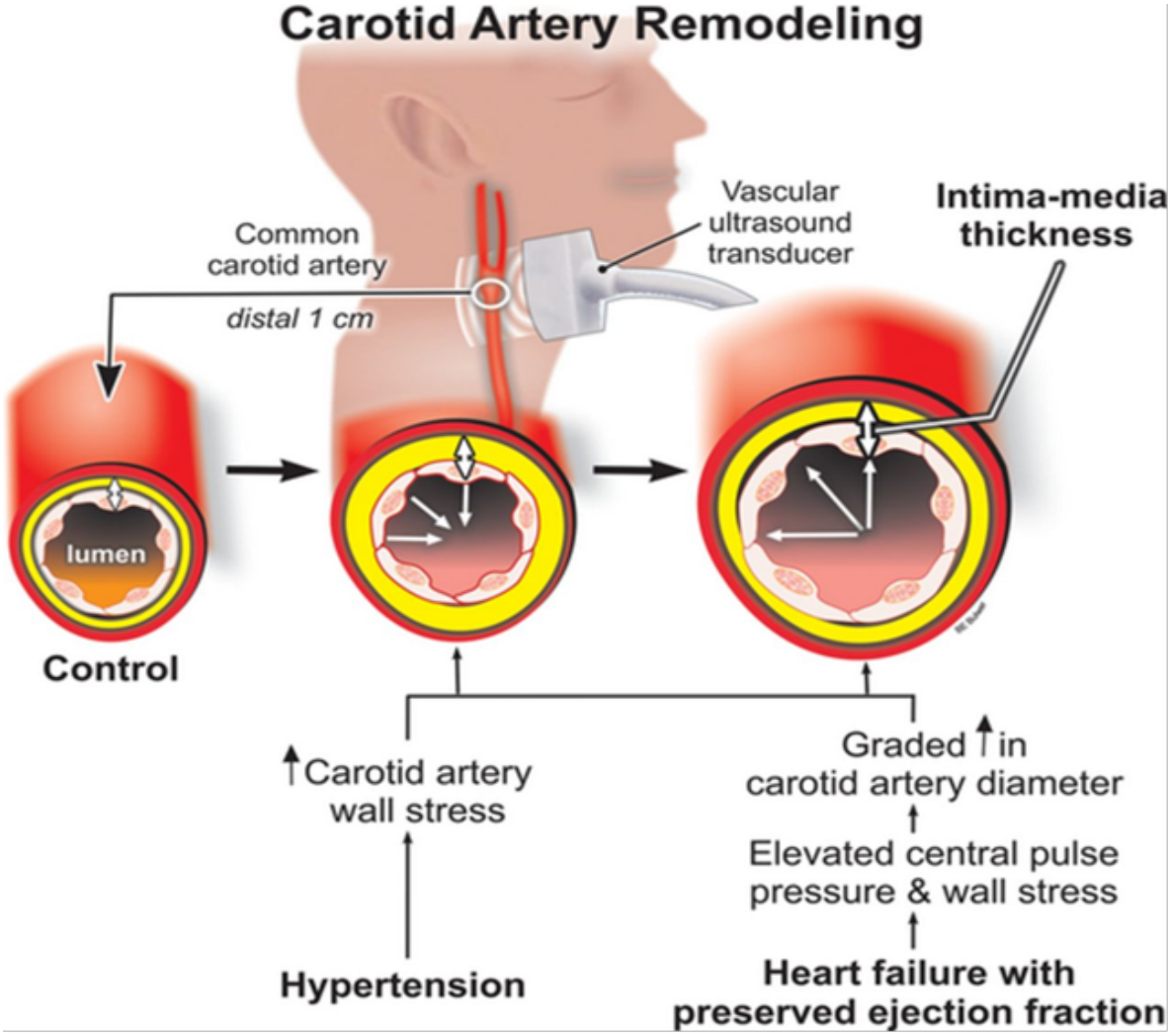

Figure 1.2: Carotid artery remodeling and failures propagating the study. Source: (Sedaghat et al., 2018)

1.2.11 Geometric Interruption

To model the geometric interruption of blood flow in the carotid artery using a novel Poiseuille-based mathematical approach, an obstruction or irregularity in the vessel geometry is intro-

duced. Assuming a scenario where there is a localized constriction or stenosis in the carotid artery. The mathematical model can be adapted to account for this geometric interruption by inclusion of the term $\left(1-\frac{R^2}{r^2}\right)$, hence the modified Poiseuille equation based on this can be written as

$$Q=\frac{\pi r_1^4 \Delta P}{8\mu L}\left(1-\frac{R^2}{r_3^2}\right) \tag{1.20}$$

when R is close to r_3, the term approaches zero, which represents the constriction in the vessel as denoted in Figure 1.4 for the swollen section.

1.2.12 Shear Stress on the velocity profile

The shear stress (τ) based on the velocity profile (u) can be derived from the modified Poiseuille equation. The shear stress (τ) near the swollen part is proposed to be influenced by the change in the cross-sectional area.

$$\begin{aligned} \tau &= \mu\tfrac{du}{dr} \\ u(r) &= \tfrac{\Delta P}{4\mu L}\left(r_1^2-r_2^2-\left[\tfrac{R^2}{3}\left(1-\tfrac{R^2}{r_3^2}\right)\right]\right) \end{aligned} \tag{1.21}$$

Proof:

Given $u(r)$:

$$\begin{aligned} u(r) &= \tfrac{\Delta P}{4\mu L}\left(r_1^2-r_2^2-\left[\tfrac{R^2}{3}\left(1-\tfrac{R^2}{r_3^2}\right)\right]\right) \\ \tfrac{du}{dr} &= \tfrac{\Delta P}{4\mu L}\left(2r_1-2r_2-\tfrac{2R^4}{3r_3^3}\right) \end{aligned} \tag{1.22}$$

Equating $\mu\frac{du}{dr}=\tau$ and solving for u yields

$$\mu\frac{du}{dr}=\overbrace{\frac{\Delta P}{2\mu L}\left(r_1-r_2-\frac{R^4}{3r_3^3}\right)}^{\mu\frac{du}{dr}}=\tau \tag{1.23}$$

The implication of the geometric interpretation and shear stress on the velocity profile is that the shear stress reduces the velocity while constriction due to geometric interruption may

change the flow pattern of the blood.

1.2.13 Proposed model

To use the Poiseuille equations to model blood flow in the carotid arteries, the basic Poiseuille equation, which describes laminar flow in a cylindrical tube, is applied. The key parameters include blood flow rate, arterial diameter, viscosity, and pressure gradient. The proposed formula for the study is from Equation (1.18). However, the proposed equation must take into account the geometric interruption and shear stress on the velocity profile.

$$Q = \frac{\pi}{8\mu L}\left(r^4\right)\left(P - \Delta P - \frac{8\mu LV}{r^2}\right) + W(r,t) \tag{1.24}$$

where Q is the volumetric flow rate; ΔP is the pressure gradient along the artery; r is the radius of the carotid artery; μ is the dynamic viscosity of blood; L is is the length of the artery and V is velocity, which is $V = u(r)$. Taking into account geometric interruption based on the proposed model diagram for the section in carotid artery is indicated in Figure 1.3 yields

$$Q = \frac{\pi r^4}{8\mu L}\left(1 - \frac{R^2}{r^2}\right)\left(P - \Delta P - \frac{8\mu LV}{r^2}\right) + W(r,t), \tag{1.25}$$

and

$$u(r) = \frac{\Delta P}{4\mu L}\left(r_1^2 - r_2^2 - \left[\frac{R^2}{3}\left(1 - \frac{R^2}{r_3^2}\right)\right]\right) \tag{1.26}$$

Therefore, the model equation for the research is given by

$$\begin{cases} Q = \frac{\pi r^4}{8\mu L}\left(1 - \frac{R^2}{r_3^2}\right)\left(P - \Delta P - \frac{8\mu LV}{r_2^2}\right) + W(r,t) \\ \quad \text{for } u(r) = \frac{\Delta P}{4\mu L}\left(r_1^2 - r_2^2 - \left[\frac{R^2}{3}\left(1 - \frac{R^2}{r_3^2}\right)\right]\right) \end{cases} \tag{1.27}$$

Viscosity of Blood (μ) is the blood viscosity can vary with hematocrit levels and temperature. Pressure Gradient (ΔP) the pressure difference between the start and end of the carotid artery segment under consideration. The blood pressure is pulsatile; therefore, the pressure

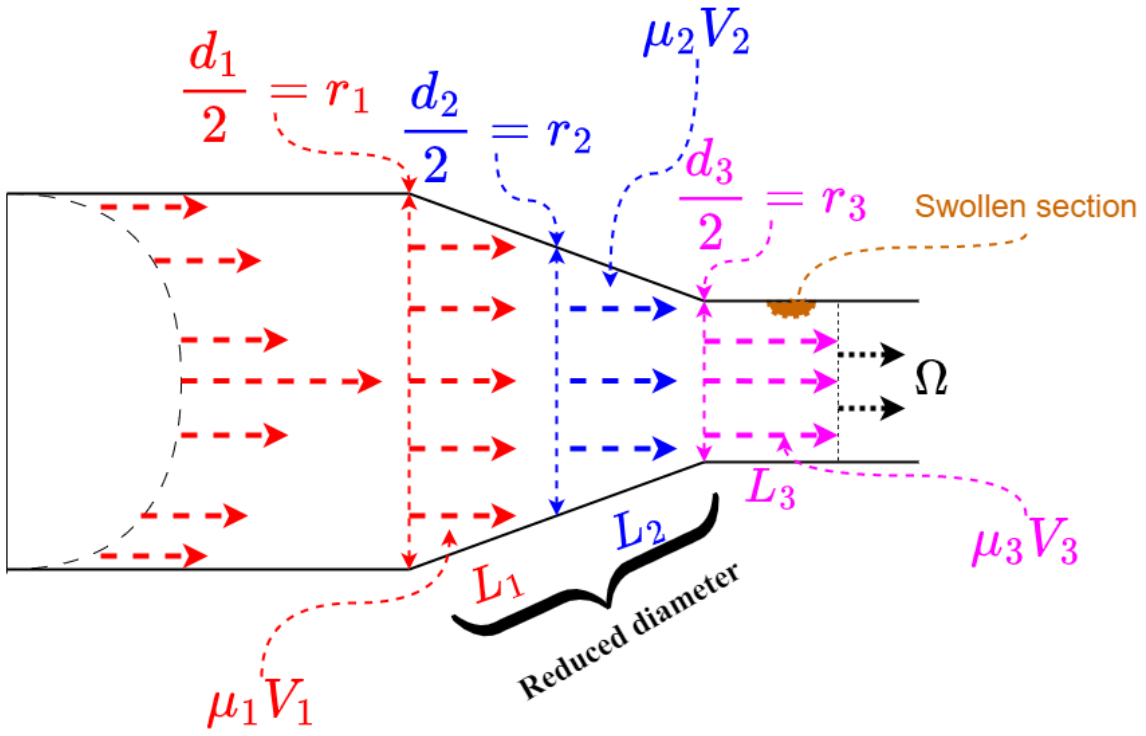

Figure 1.3: The model diagram for the research.
Source: Researcher, 2023.

gradient can vary during the cardiac cycle. Thus, in this proposed research, the pulsatility of the pressure gradient will also be considered in the modelling. Length of the Artery (L) measures the length of the carotid artery segment. This will vary depending on the specific section of the carotid artery. The term $R^2/3(1-R^2/(r_3^2))$ in the velocity profile u(r) represents a modification to the Poiseuille flow to account for a constriction or swollen section in the artery. This term introduces a radial dependence on the velocity, influencing the flow near the swollen section (Fig. 1.3). The specific conditions leading to this term are associated with the geometry of the artery and the presence of a swollen section. The swollen section modifies the flow profile, and this modification is incorporated into the velocity equation. The parameter R represents the size or dimension of the swollen section. The term $R^2/(r_3^2)$ is a dimensionless ratio that varies with radial position r_3 within the artery. As R approaches r_3, the ratio $R^2/(r_3^2)$ approaches 1. This means that near the swollen section $(r_3 \approx R)$, the term $1 - R^2/(r_3^2)$ approaches 0. The scenario is presented in Figure 1.4.

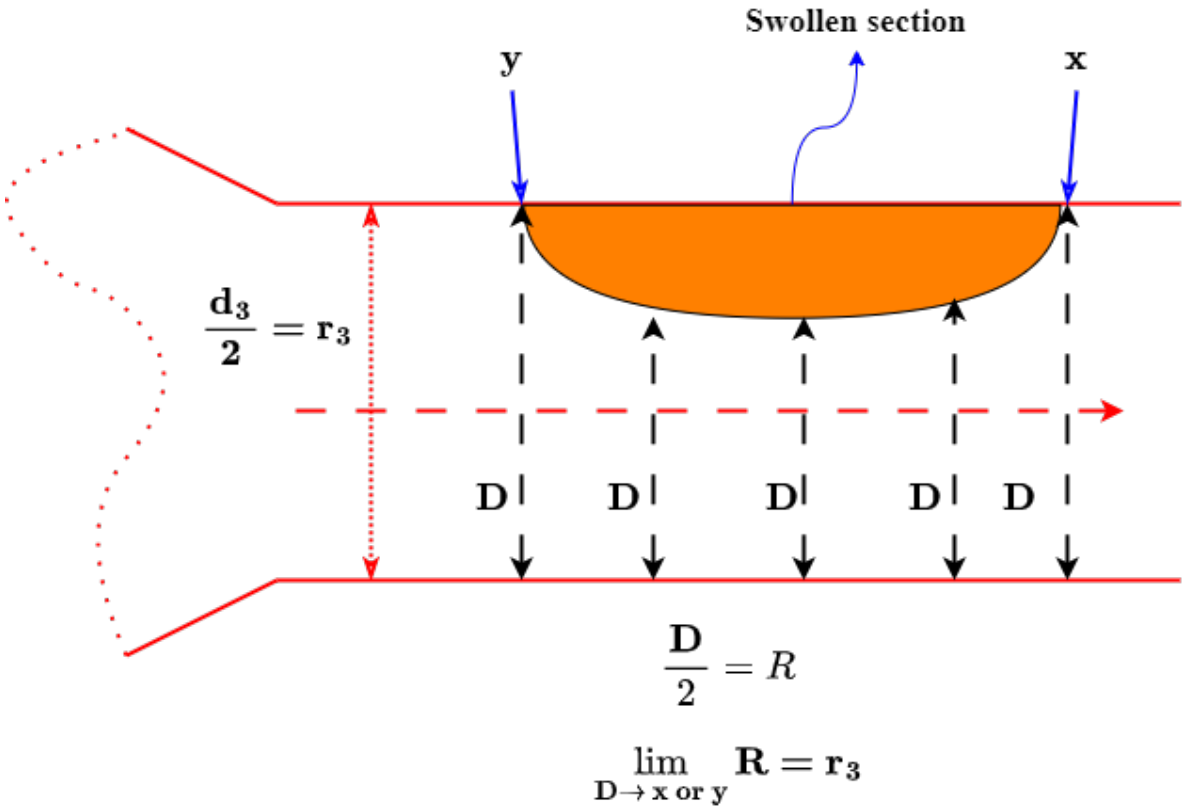

Figure 1.4: Details about the swollen sections.
Source: Researcher, (2023).

The term $R^2/3(1 - R^2/(r_3^2))$ is designed to introduce a decrease in velocity near the swollen section. The factor $R^2/3$ determines the magnitude of this influence. The term $R^2/3(1 - R^2/(r_3^2))$ also ensures a smooth transition in velocity as R shifts from the centre towards x or y until $(R \approx r_3)$.

1.2.14 Basic assumptions

The following assumptions guide the research:

(i) The model will assume that blood is an incompressible fluid, meaning its density remains constant. While blood is not strictly incompressible, this assumption is often made to simplify the equations.

(ii) The model may assume axisymmetry, which simplifies the problem to a two-dimensional

representation.

(iii) The model will assume that blood flow at the artery's inlet is laminar and without turbulence.

1.3 Statement of the Problem

The Poiseuille equations have long been applied in modeling blood flow due to their effectiveness in describing laminar flow through cylindrical tubes (Nichols, 2022). In this study, their applicability was investigated within the context of large and medium-sized arteries, particularly the carotid artery, where laminar flow conditions typically prevail under physiological states. The fundamental assumptions underlying the Poiseuille equations—namely incompressible, Newtonian, and steady, state flow—are generally valid for vessels exhibiting low Reynolds numbers, making them suitable for modeling hemodynamic behavior in many arterial systems. Arteries such as the carotid possess approximately cylindrical geometries, and blood, being nearly incompressible, behaves as a Newtonian fluid within certain shear rate ranges. These properties justify the use of Poiseuille-based models to represent steady laminar flow. However, the simplifications inherent in the Poiseuille formulation neglect several essential characteristics of physiological blood flow, particularly under disturbed or pathological conditions.

This research addressed these limitations by evaluating the performance of the Poiseuille-based model under non-ideal flow conditions, specifically those involving turbulence, pulsatility, and complex arterial geometries. Although the Poiseuille equation provides accurate results under laminar flow, the study revealed its reduced reliability when applied to pulsatile and disturbed flows commonly observed in stenosed or bifurcated carotid arteries. Such flow disturbances cause irregular velocity distributions, elevated wall shear stress, and deviations from the linear relationships assumed by the classical model.

The study identified and resolved three major gaps in the literature. First, there has been limited understanding of the effects of vascular shear stress under turbulent or stenotic condi-

tions. The Poiseuille equation assumes smooth, laminar flow, whereas in practice, disturbed flow in the carotid artery often exhibits turbulence and flow reversal (Montorfano et al., 2020). Second, the equation assumes steady-state conditions, neglecting the pulsatile nature of blood flow driven by cardiac cycles. This pulsatility significantly affects flow velocity and wall shear stress, influencing overall hemodynamic stability (Montorfano et al., 2020). Third, the geometry of the carotid artery, including bifurcations and localized narrowing, substantially impacts blood flow behavior. Traditional Poiseuille models, which simplify geometry as uniform and cylindrical, fail to capture these effects accurately (Lopes et al., 2020).

To overcome these challenges, the study introduced an extended form of the Poiseuille equation, as shown in Equation (1.18), incorporating additional terms to account for flow resistance, pulsatility, and pressure losses beyond classical laminar assumptions. The modified formulation integrated parameters such as velocity V, fluid density ρ, and frictional losses due to vascular geometry and dynamic wall interactions. This enhanced model provided a more realistic representation of blood flow in arteries exhibiting non-laminar behavior. Computational Fluid Dynamics (CFD) simulations conducted in MATLAB, using a Finite Volume Method (FVM) approach, demonstrated that arterial narrowing significantly increased vascular stress and reduced flow rate, especially under pulsatile flow conditions. These results validated the refined model and underscored the limitations of traditional Poiseuille formulations in capturing complex hemodynamic phenomena. The findings of this study highlight the necessity of adopting more advanced modeling frameworks that incorporate turbulence, pulsatility, and geometric variability to improve the predictive accuracy of blood flow analysis and support clinical decision-making in cardiovascular disease assessment.

1.4 Objectives

1.4.1 General objective

The study models the impact of geometric interruption, vascular stress, and pulsatility on blood flow calculation in the carotid artery during accidents.

1.4.2 Specific objectives

(i) To develop a modified Poiseuille-based mathematical model for blood flow in the pulsatile carotid artery.

(ii) To investigate the impact of geometric interruption of blood flow on carotid artery for a novel Poiseuille-based mathematical model.

(iii) To evaluate the influence of vascular stress and pulsatility on blood flow on carotid artery for a novel Poiseuille-based mathematical model.

1.5 Significance of the study

Understanding the behavior of blood flow during accidents is crucial for the medical field. It can provide insights into how traumatic events, such as car accidents or injuries, affect blood flow in the carotid artery. This knowledge is vital for diagnosing and treating injuries, as well as improving patient outcomes. Modeling blood flow during accidents can help assess the severity and type of injuries to the carotid artery. This information is critical for medical professionals to make informed decisions about treatment and intervention. Developing patient-specific models allows for personalized medical treatment. By using individual data, including the geometry of the carotid artery and patient-specific parameters, medical professionals can better predict the consequences of accidents and tailor treatment accordingly. Such studies contribute to the field of biomechanics, which explores the mechanical aspects of biological systems. Understanding the biomechanics of blood flow during accidents can lead to improved safety measures and vehicle design, reducing the risk of injuries. Insights gained from these studies can inform safety standards, such as vehicle safety design and road engineering.

The knowledge of how accidents impact blood flow can lead to the development of safety mechanisms that reduce the risk of carotid artery injuries. Modeling blood flow during accidents can aid in the development of intervention strategies for trauma patients. This can

include devising emergency medical procedures and equipment designed to mitigate the effects of carotid artery injuries. Computational modeling of blood flow is a growing field that integrates medical knowledge with engineering and computational techniques. It represents an interdisciplinary approach to improving medical care and patient outcomes. These models can be used for educational purposes, training medical professionals and first responders better to understand the physiological consequences of accidents and injuries. Understanding the dynamics of blood flow in the carotid artery following an accident is important for predicting and evaluating post-injury outcomes, including the potential for long-term complications. Research in this area often involves collaboration between medical professionals, engineers, and mathematicians. Such interdisciplinary work can lead to innovative solutions and a more comprehensive understanding of trauma and its effects on the human body.

CHAPTER TWO

LITERATURE REVIEW

2.1 Introduction

The chapter presents theoretical review for the research. Later sections of the chapter present the empirical review of the existing works for the research gap.

2.2 Theoretical Review

The mathematical theoretical formulation of modeling blood flow can be approached through various methods. One common approach is to use the Navier-Stokes equations and the continuity equation to describe the flow of blood as a Newtonian fluid through the circulatory system (Khalid et al., 2021). Another approach is to consider blood as a non-Newtonian fluid with its viscosity as a function of the hematocrit, plasma viscosity, and shape factor of the red blood cells, and model the flow using the Power-law fluid model (Rao and Mishra, 2004) or the Prandtl fluid model (Karthik et al., 2022).

Theoretical models for regulation of blood flow take into account the combined effects of multiple interacting mechanisms, including sensitivity to pressure, flow rate, metabolite (Any substance involved in metabolism (either as a product of metabolism or as necessary for metabolism)) levels, and neural signals (Claassen et al., 2021). These models provide quantitative descriptions of the mechanisms involved in blood flow regulation and show how these mechanisms interact in networks of interconnected vessels. This is because blood flow modeling plays a significant role in understanding hemodynamics, influencing areas such as medical diagnostics, treatment, and biomedical engineering. Theoretical modeling of blood flow

can be approached through different methods, primarily rooted in fluid dynamics.

2.3 Empirical Review

Hameed et al. (2023) compared blood flow patterns in diseased and treated carotid artery bifurcations for improved cardiovascular disease diagnosis and treatment. They employed computational fluid dynamics (CFD) analysis of simulated blood flow in models with and without stenosis and stenting. Control volume discretization and measured blood flow rates were also used. The transition from turbulent to laminar flow was observed post-stenosis, with distinct comparisons at four downstream locations. The results indicated that stenosed carotid arteries exhibited high wall shear stress, irregular flow, and low pressure, oscillating velocity and pressure profiles. Stented models showed minimal pressure, velocity, and wall shear stress fluctuations, maintaining laminar flow. The research findings support the research since it recommends that until carotid artery abnormalities are resolved, establishing a foundation for optimized stent design to restore normal blood flow is crucial, and further research is crucial.

Fojas and De Leon (2013) developed a 2D computational representation of the carotid artery, and its bifurcation using computational software. The model employed the Arbitrary Lagrangian Eulerian technique for numerical simulations. The carotid artery's structure was derived from CT scans through computer-aided design, and blood behavior was simulated as an incompressible Newtonian fluid. The study applied a Eulerian reference for the blood domain, combined with the Lagrangian approach for the structural domain, enabling the numerical modeling of hemodynamics using 2D axially symmetric incompressible Navier-Stokes equations. Simulation results were compared with blood velocity data obtained from Doppler ultrasound measurements.

Singh and Singh (2022) research analyzed the intricate blood flow within a 2D model of the human carotid artery. Analysis System (ANSYS) 19.1 software simulates steady blood flow in a 2D carotid artery bifurcation model, employing the finite volume method on a staggered

grid with the control volume approach. The study focuses on key hemodynamic parameters such as blood velocity, assuming blood behaves as a Newtonian and incompressible fluid. The governing equation for the model is the incompressible 2D Navier-Stokes equation. The flow analysis reveals two distinct patterns: laminar flow before the artery bifurcation due to the regular design and turbulent or reverse flow post-bifurcation, caused by an irregular flow pattern resulting from a change in shape.

Fusi and Farina (2020) investigated the linear stability of unidirectional Poiseuille flow of blood, treating the fluid as spatially inhomogeneous, where viscosity varied with red blood cell (RBC) concentration. The focus was on small blood vessels, such as terminal branches of arteries, arterioles, or venules, where RBCs are unevenly distributed across the vessel cross-section. A classical normal-mode linear analysis was used for the stability assessment, resulting in a fourth-order eigenvalue problem, which was solved numerically. The findings revealed that the flow was unconditionally unstable. However, in cases where RBC concentration decreased toward the vessel walls, the instability grew at such a slow rate that it would take a significantly long time for the instability to become observable. In contrast, when RBCs were more concentrated near the vessel walls, the growth rates of the instability were at least three orders of magnitude higher. Thus, the study suggested that RBC distributions concentrated near the center of the vessel could be considered more stable compared to those where RBCs accumulated towards the walls.

Dhange et al. (2022b) explored the effects of arterial stenosis, a common cardiovascular condition that restricts blood flow, on blood flow dynamics in an inclined artery with stenosis followed by an expansion (widening). The primary aim was to analyze blood flow through this system under the influence of a constant, incompressible Casson fluid—a non-Newtonian model—subjected to a magnetic field. Analytical expressions for surface shearing stress, pressure drop, flow resistance, and velocity were derived using a mild stenosis approximation. The study investigated how various physical parameters affected flow impedance, velocity, and surface shearing stress. It was found that, due to the non-Newtonian properties

of the Casson fluid, surface shearing stress decreased while flow impedance increased. Furthermore, as the severity of stenosis increased, both flow resistance and shearing stress rose, while both factors diminished with the degree of expansion. These results provide insights into the behavior of blood flow in stenotic vessels, particularly highlighting the influence of vessel constriction and dilation on key hemodynamic parameters.

Sarifuddin (2022) investigated the effects of stenosis and mass transfer on arterial blood flow using a mathematical model. Blood was modeled as a non-Newtonian fluid following the Casson model, while the arterial wall was treated as axisymmetric, with the stenosis outline derived from a casting of a mildly stenosed artery. Mass transfer within the blood was governed by the convection-diffusion equation. The governing equations of motion were numerically solved using the Marker and Cell method, with results checked for numerical stability and accuracy. The research examined the effects of two different stenosis models, varying stenosis severity, and different yield stress parameter values. Special attention was given to the influence of stenosis on wall shear stress and the Sherwood number, and the outcomes were presented graphically. The results showed consistency with several existing studies, confirming the model's reliability in simulating the impact of stenosis on arterial flow and mass transfer, thus validating its applicability.

Wang (2022) focused on the development of a new model to simulate haemorrhagic transformation (HT), a common complication following ischaemic stroke due to damage to the blood-brain barrier (BBB). HT can occur either as a result of stroke progression or as a complication of reperfusion therapy, leading to bleeding in the brain and potentially worsening the brain tissue damage, thus increasing the risk of disability or death. Given the global rise in cerebrovascular diseases, including stroke, this work aimed to provide a more effective way of understanding and predicting HT. The proposed model was developed in three stages. First, a mathematical model of HT was created to simulate the consequences of HT over different vasculature length scales. In the second phase, this model was expanded into a larger, multi-scale microvasculature model to study the effects of HT on surrounding tissue

and vasculature. Finally, the model was applied to a whole-brain computational framework, incorporating effects such as capillary compression and tissue displacement. For validation, the model examined the volume of haematoma in 15 subjects and compared the findings with clinical imaging data. Additionally, perfusion levels in the region affected by HT were calculated and compared with experimental data. This model was the first of its kind to simulate the correlation between bleeding regions and haematoma formation, potentially aiding clinicians in assessing HT in future clinical settings.

Csippa (2023) explored the field of blood rheology, focusing on the complexities of blood flow behavior, which is crucial for understanding both physiological and pathological conditions. Various rheological models were reviewed, ranging from Generalized Newtonian models to more advanced thixotropic and elastoviscoplastic models. Among these, the Horner-Armstrong-Wagner-Beris (HAWB) model provided valuable insights into the interaction between reversible and irreversible phenomena in blood flow. Additionally, the recent development of the modified HAWB (mHAWB) framework offered improved accuracy and versatility for modeling blood rheology, with promising applications in diagnostics and therapeutics. Microscopic and mesoscopic simulations were also highlighted as they helped bridge the gap between theoretical models and experimental findings, offering deeper insights into blood behavior. Furthermore, multiscale models were discussed as a promising method to capture the complexities of blood rheology across various length scales. The clinical significance of blood rheology was examined in relation to conditions such as polycythemia, neonatal respiratory distress, and circulatory inadequacy. By gaining a comprehensive understanding of blood rheology, this research contributed to advancing knowledge of blood flow dynamics and its potential applications in healthcare.

Wang (2023) noted that the primary purpose of the heart and lungs is to maintain blood circulation, delivering oxygen (O_2) and other nutrients to cells while removing metabolic waste products, such as carbon dioxide (CO_2). In open-heart surgery, cardiopulmonary bypass (CPB) is often employed to isolate the heart and lungs, temporarily assuming their func-

tion during aortic cross-clamping. This provides a quiet, bloodless environment conducive to performing the surgical procedure. CPB technology typically involves an oxygenator, venous/cardiotomy reservoir, pumps (roller or centrifugal), filters, tubing, and cardiotomy suction devices. In contrast, extracorporeal life support (ECLS), a modified form of CPB, is used in cases of severe heart and/or lung failure. This includes different forms of extracorporeal membrane oxygenation (ECMO), such as venoarterial (VA), venovenous (VV), and venovenoarterial (VVA) ECMO, as well as extracorporeal carbon dioxide removal $(ECCO_2R)$, which can be implemented in venovenous (VV) or arteriovenous (AV) configurations. ECMO systems take over part of the heart and lung function for extended periods, allowing these organs to rest and recover. This support can serve as a bridge to recovery, long-term ventricular assist devices (VAD), heart or lung transplantation, or as destination therapy for patients with irreversible organ failure.

Tigges (2023) noted that bleeding-related complications often result in extended hospital stays and can be fatal. In both Germany and the United States, excessive blood loss is a leading cause of death in civilian accidents, particularly among individuals under 45 years of age. However, there is currently no routinely available patient monitoring system that can quickly and reliably assess circulating blood volume and cardiovascular status. The study aimed to advance non-invasive detection of hypovolemia by exploring new approaches, leveraging advancements in sensor technology, signal processing, and machine learning techniques. The central focus was on the robust acquisition and integrated processing of multimodal biosignals. To address this, a wireless sensor network was developed, featuring high-performance sensor nodes with efficient analog front-ends. These were designed to function effectively in challenging environments. Accurate synchronization within the network was critical for joint signal analysis, and an algorithm was created to achieve this high synchronization accuracy, facilitating biosignal data transmission for monitoring and real-time processing. Additionally, a novel method of statistical signal fusion was introduced, enhancing the detection of cardiac activity reference points across large sets of signals. This involved extending Hidden Markov

modeling and developing a refined Viterbi algorithm for optimal identification of heartbeat positions. A multimodal classification method for non-invasive detection of hypovolemia was also developed, based on data collected from a lower-body negative pressure study. Various physiological parameters, including pulse wave morphology, pulse timings, heart rate variability, and respiration, were analyzed to observe compensatory mechanisms during simulated progressive central hypovolemia. Machine learning techniques were applied to these data, resulting in innovative multimodal approaches to patient monitoring. The results demonstrated that combining advanced sensor networks with machine learning methods provided a comprehensive means to detect and monitor hypovolemic states non-invasively, potentially addressing the current gap in rapid and reliable cardiovascular monitoring.

Ellis and Joshi (2025) noted that understanding the physiology of cerebral and spinal cord circulation is critical in neuroanesthesia practice. Given the limited progress in neuroprotective pharmacology, the modulation of cerebral and spinal cord blood flow, sometimes accompanied by hypothermia, remains a primary intervention that may influence clinical outcomes. Perioperative management of neurological conditions, such as brain aneurysms, arteriovenous malformations, moyamoya disease, traumatic brain and spinal cord injuries, cerebral vasospasm, and stroke, necessitates a deep understanding of the vascular physiology of the brain and spinal cord. Research on cerebral circulation has advanced knowledge of central nervous system (CNS) function and its pathophysiology. This chapter aimed to review the fundamental mechanisms that govern CNS circulatory dynamics and the tools used to investigate them. The chapter began with an overview of the regulation of cerebral blood flow (CBF) in healthy individuals and the disruption of this regulation in disease states. Various methodologies for measuring CBF were then examined. Following this, spinal cord blood flow was discussed, before concluding with the practical aspects of manipulating cerebral blood flow and monitoring it in clinical settings. The findings demonstrated that understanding and controlling cerebral and spinal cord circulation play a pivotal role in improving clinical outcomes in neuroanesthesia. The methodologies and interventions reviewed offered valuable insights

into the management of CNS blood flow in both health and disease.

2.3.1 Summary of literature review

Hameed et al. (2023) compare blood flow patterns in stenosed and treated carotid artery bifurcations, providing insights relevant to the development of a Poiseuille-based mathematical model for pulsatile blood flow. Their use of computational fluid dynamics (CFD) and control volume analysis highlights how high wall shear stress, oscillating velocity profiles, and irregular flow characterize stenosed arteries, whereas stented models exhibit restored laminar flow and reduced fluctuations. This study emphasizes the importance of designing interventions that normalize blood flow dynamics, aligning with the objective to develop a new model for pulsatile flow in the carotid artery, which could guide optimized stent designs.

Fojas and De Leon (2013) and Singh and Singh (2022) investigate hemodynamic parameters in carotid artery models, highlighting how bifurcation geometries lead to disruptions in blood flow. These studies used 2D computational simulations and demonstrated that bifurcations cause reverse or turbulent flow post-bifurcation. Their findings align with the second objective of the research, which seeks to analyze the impact of geometric interruptions in the carotid artery on the newly developed Poiseuille-based model. Such geometric features profoundly influence flow patterns and could be critical to understanding pathological blood flow behaviors.

Fusi and Farina (2020) and Dhange et al. (2022b) explored the effects of blood viscosity variations and non-Newtonian fluid properties on blood flow in stenosed vessels. These studies provide valuable insights into the hemodynamic changes caused by arterial constrictions and expansions, with implications for stress on vascular walls. They support the third objective of investigating how vascular stress and blood pulsatility affect flow in the carotid artery, emphasizing the role of wall shear stress and flow resistance, critical factors in stenotic arteries and informing the development of a more realistic Poiseuille-based model.

Sarifuddin (2022) and Csippa (2023) focused on blood rheology and the effects of stenosis

on mass transfer and blood dynamics, using advanced mathematical models. Their findings align with the necessity of developing accurate models that account for non-Newtonian blood properties and yield stress in arterial walls. These studies highlight research gaps in simulating blood pulsatility and vascular stress in realistic conditions, supporting the third objective, which aims to incorporate these factors into the novel Poiseuille-based model. Improved understanding of these dynamics is crucial for accurate simulations of stenotic and healthy arterial conditions.

2.3.2 Research Gap

The studies reviewed explore various aspects of blood flow modeling in the carotid artery, highlighting the importance of fluid dynamics in cardiovascular health. Hameed et al. (2023) examined the differences in blood flow between diseased and treated carotid arteries using computational fluid dynamics (CFD), revealing that stenosed arteries exhibit high wall shear stress and irregular flow patterns, while stented arteries restore laminar flow. Similarly, Fojas and De Leon (2013) and Singh and Singh (2022) analyzed blood velocity and hemodynamics in carotid artery bifurcations, noting distinct transitions between laminar and turbulent flows. These studies contribute to understanding flow dynamics but leave a gap in developing a mathematical model that integrates the effects of pulsatility and arterial geometry.

In addressing the impact of geometric interruptions on blood flow, Dhange et al. (2022b) explored the effects of stenosis and vessel expansion on blood flow resistance and wall shear stress using a non-Newtonian Casson fluid model. Their results emphasize the role of vessel constriction in increasing flow impedance and surface stress. While useful, these findings lack integration into a pulsatile flow model relevant to real-world carotid artery geometries. Similarly, Sarifuddin (2022) used a non-Newtonian model to analyze stenosis effects but did not consider the dynamic nature of blood flow under varying pulsatile conditions, leaving room for further exploration.

Finally, studies by Fusi and Farina (2020) and Wang (2022) introduced microvascular models

to understand blood flow behavior and the instability of blood viscosity due to red blood cell concentration. However, these studies primarily focus on microvessels and do not directly address the macroscopic impact of vascular stress or pulsatility on the carotid artery. This gap highlights the need for a novel Poiseuille-based model that captures the complex interaction between pulsatile blood flow, arterial stress, and carotid geometry in larger vessels. The research gap is outlined systematically in Table 2.1.

Table 2.1: Summary of research studies with gaps related to a novel Poiseuille-based mathematical model for blood flow in the pulsatile carotid artery.

Author	**Research Findings**	**Literature Gap**
Hameed et al. (2023)	Stenosis led to irregular flow and high wall stress; stenting restored laminar flow	Geometric effects of flow interruption remain unexplored
Fojas and De Leon (2013)	Navier-Stokes equations simulated hemodynamics, with validation from Doppler data	Impact of vascular stress on pulsatile blood flow remains unclear
Singh and Singh (2022)	Regular design led to laminar flow; irregularities caused turbulent flow post-bifurcation	Investigation of pulsatile flow and vascular stress is needed
Fusi and Farina (2020) Dhange et al. (2022b)	RBC concentration near vessel walls increased flow instability Stenosis increased flow resistance; Casson fluid reduced wall shear stress	Lack of geometric influence on flow in pulsatile arteries Need for pulsatile blood flow modeling in carotid arteries
Sarifuddin (2022)	Stenosis influenced shear stress and Sherwood number in blood flow	No focus on geometric impact in pulsatile carotid arteries
Wang (2022)	HT model predicted hematoma volume and perfusion changes	Geometric interruptions in pulsatile flow unaddressed

Author	Research Findings	Literature Gap
Csippa (2023)	Improved blood rheology modeling with HAWB framework	Need for a Poiseuille-based model incorporating blood pulsatility
Wang (2023)	ECMO systems restored blood flow in failing organs	Impact of pulsatility in carotid artery on Poiseuille-based flow remains unexamined
Tigges (2023)	Machine learning enhanced non-invasive cardiovascular monitoring	Lack of geometric effects and vascular stress modeling
Ellis and Joshi (2025)	Blood flow control improved outcomes in brain and spinal injuries	Further investigation into carotid artery stress and pulsatile flow needed

Despite extensive modeling efforts, gaps remain in accounting for pulsatile flow, turbulent effects, and geometric interruptions in the carotid artery. This study addresses these by introducing a modified Poiseuille-based model.

2.3.3 Current Knowledge

Blood flow in the carotid artery is significantly influenced by arterial abnormalities such as stenosis and post-treatment conditions. Hameed et al. (2023) compared blood flow patterns in stenosed and stented carotid arteries to improve the diagnosis and treatment of cardiovascular diseases. Their study employed Computational Fluid Dynamics (CFD) simulations to analyze velocity, pressure, and wall shear stress in different models. The results indicated that in stenosed arteries, turbulence dominated due to abrupt geometric interruptions, leading to high wall shear stress and oscillating velocity profiles. This aligns with the limitations of the Poiseuille equation, which assumes a smooth, laminar flow that does not accurately account for turbulent effects in post-stenotic regions. Post-treatment stented models showed reduced fluctuations, maintaining more stable flow conditions, emphasizing the necessity of advanced

hemodynamic models beyond the basic Poiseuille framework.

Computational modeling plays a critical role in understanding hemodynamics in complex arterial geometries. Fojas and De Leon (2013) developed a 2D computational representation of the carotid artery using numerical simulations based on the Navier-Stokes equations. Their Arbitrary Lagrangian-Eulerian (ALE) approach incorporated arterial geometry derived from CT scans, which provided insights into real-world blood flow patterns. The study confirmed that Poiseuille's assumptions hold true primarily in straight arterial segments but fail in regions of bifurcation or sudden constriction, where secondary flow effects and vortices develop.

Similarly, Singh and Singh (2022) analyzed blood flow dynamics in a 2D carotid artery bifurcation model using finite volume methods. Their study highlighted the transition from laminar to turbulent flow post-bifurcation, reinforcing that the Poiseuille equation alone is insufficient in regions where arterial geometry changes abruptly. The findings indicated that while the equation is useful for predicting steady-state flow, pulsatile dynamics and turbulent effects require more advanced models incorporating Navier-Stokes equations.

Blood is a complex, non-Newtonian fluid whose rheological properties impact flow stability, especially in geometrically interrupted vessels. Fusi and Farina (2020) investigated the linear stability of unidirectional Poiseuille flow in small arteries by incorporating red blood cell (RBC) concentration variations. Their findings demonstrated that viscosity variations due to RBC aggregation significantly affect stability, with instability growth rates varying based on cell distribution. In larger arteries such as the carotid, this suggests that abrupt geometric changes could exacerbate instability, challenging the validity of Poiseuille-based models.

The effects of arterial stenosis on hemodynamics were further examined by Dhange et al. (2022b), who modeled blood flow as a Casson fluid in a stenosed artery under a magnetic field. Their analysis of surface shear stress, pressure drop, and velocity profiles highlighted increased flow impedance in stenotic regions, conditions where the classical Poiseuille equation does not provide accurate predictions. These findings reinforce the necessity of extend-

ing Poiseuille models to incorporate non-Newtonian blood behavior and stenosis-induced perturbations.

Sarifuddin (2022) studied mass transfer and stenosis effects on arterial blood flow using a mathematical model based on the Casson fluid. Their findings showed that stenosis severity influenced shear stress and the Sherwood number, which governs mass transfer rates. The presence of stenosis disrupted Poiseuille flow assumptions, as increased yield stress parameters altered shear stress distribution, leading to significant deviations from the predicted laminar behavior.

Recent advancements in hemodynamic modeling focus on multi-scale representations that integrate microvascular dynamics with larger arterial networks. Wang (2022) developed a model for hemorrhagic transformation following ischemic stroke, highlighting how arterial damage affects systemic and microcirculatory flow. Their work underscores the importance of incorporating localized geometric interruptions into broader circulatory models to improve predictive accuracy.

Similarly, Csippa (2023) reviewed rheological models of blood flow, including Newtonian and non-Newtonian frameworks, emphasizing that thixotropic and elastoviscoplastic models better capture the complexities of blood behavior. These studies suggest that while the Poiseuille equation remains a fundamental starting point, enhanced models incorporating multi-scale dynamics and variable viscosity are essential for accurately simulating post-accident carotid artery flow.

The importance of accurately modeling arterial blood flow extends to clinical applications such as extracorporeal circulation and cardiovascular monitoring. Wang (2023) reviewed cardiopulmonary bypass and extracorporeal life support technologies, noting that controlled blood flow mechanics are crucial in surgical and emergency medicine. Similarly, Tigges (2023) explored non-invasive detection methods for hypovolemia using machine learning and sensor networks, which rely on accurate hemodynamic models.

Neurovascular dynamics were further examined by Ellis and Joshi (2025), who discussed the

physiological modulation of cerebral and spinal cord circulation. Their research emphasized that interventions such as hypothermia and controlled blood flow adjustments rely on predictive models, reinforcing the need for refined equations beyond Poiseuille's assumptions.

CHAPTER THREE

METHODOLOGY

3.1 Introduction

The chapter presents the details of the main variables of the study, namely geometric interruption, pulsatility and vascular shear stress.

3.2 Mathematical Formulation

3.2.1 Finite Volume Method

The Finite Volume Method (FVM) is a widely used numerical approach for solving partial differential equations, especially in fields where the conservation of physical quantities such as mass, momentum, and energy is critical (Van Hoecke et al., 2023). This makes it particularly well-suited for fluid dynamics, heat transfer, combustion, and related applications where integral conservation laws are more naturally applied than differential formulations.

Unlike the Finite Element Method (FEM), which employs test functions and weak formulations, or the Finite Difference Method (FDM), which approximates derivatives at discrete points, the FVM divides the computational domain into a finite number of small control volumes (or cells). The governing equations are then integrated over each control volume, and fluxes are computed across the faces of these volumes. This approach ensures that the conserved quantities remain balanced across the domain, even in the presence of shocks, discontinuities, or complex boundary conditions.

An important advantage of the FVM is its strong conservation property (Zhang and Wang,

2024). Because the method is based on the integral form of the conservation equations, the numerical fluxes computed at the interfaces of control volumes ensure exact local conservation. This feature is essential in cardiovascular modeling, where minor deviations in mass or momentum conservation can propagate into significant errors over time and space, particularly in pulsatile or disturbed flow conditions.

FVM handles complex geometries and irregular meshes effectively, making it an ideal choice for modeling blood flow in arteries such as the carotid, which may exhibit bifurcations, stenotic regions, or non-cylindrical cross-sections. It can also accommodate discontinuities in the solution, which are common in flows with abrupt geometric transitions or variable wall properties.

In the present study, the FVM was implemented using structured grids where the governing Navier–Stokes equations, were modified to include geometric drag and pulsatile effects through a Womersley function, were discretized using the control volume approach. The convective and diffusive fluxes were computed at the faces of each control volume using central difference schemes, and temporal integration was carried out using an explicit time-stepping method. Boundary conditions were applied based on physiological assumptions, including no-slip conditions at the arterial wall and pulsatile inflow velocity profiles representative of systolic and diastolic phases.

The Finite Volume Method provided a robust and accurate framework for simulating unsteady, pulsatile blood flow in geometrically interrupted arterial segments. Its ability to conserve flow quantities while resolving complex flow phenomena made it the most appropriate choice for this investigation.

3.2.2 Gauss–Legendre Quadrature

Gauss–Legendre quadrature is a numerical integration technique that employs optimally chosen nodes and weights to accurately approximate the definite integral of a function. It is particularly efficient for smooth integrands and outperforms simpler techniques, such as the

trapezoidal and Simpson's rules, especially for higher-degree polynomials (Johansson and Mezzarobba, 2018).

The standard Gauss–Legendre quadrature approximates the integral of a function $f(x)$ over the interval $[-1, 1]$ as:

$$\int_{-1}^{1} f(x)\,dx \approx \sum_{i=1}^{n} w_i f(x_i), \tag{3.1}$$

where n is the number of quadrature points, x_i are the nodes (i.e., the roots of the Legendre polynomial $P_n(x)$), and w_i are the corresponding weights. The nodes are defined by the equation:

$$P_n(x_i) = 0, \tag{3.2}$$

where $P_n(x)$ is the Legendre polynomial of degree n, which can be expressed explicitly as:

$$P_n(x) = \frac{1}{2^n n!} \frac{d^n}{dx^n} \left[(x^2 - 1)^n \right]. \tag{3.3}$$

These polynomials are orthogonal with respect to the weight function $w(x) = 1$ over $[-1, 1]$, which ensures numerical stability and accuracy in integration. The weights w_i are computed using:

$$w_i = \frac{2}{(1 - x_i^2)\left[P_n'(x_i)\right]^2}, \tag{3.4}$$

where $P_n'(x)$ denotes the derivative of $P_n(x)$ with respect to x.

For integrals over an arbitrary interval $[a, b]$, the method requires a change of variables to map the interval to $[-1, 1]$. This is accomplished using the linear transformation:

$$t = \frac{2x - (b + a)}{b - a}, \quad \text{or equivalently,} \quad x = \frac{(b - a)t + (b + a)}{2}. \tag{3.5}$$

Applying this substitution, the integral becomes:

$$\int_a^b f(x)\,dx = \frac{b-a}{2}\int_{-1}^{1} f\left(\frac{(b-a)t+(b+a)}{2}\right)\,dt. \tag{3.6}$$

This transformed integral can then be approximated using the Gauss–Legendre quadrature rule over $[-1, 1]$. The quadrature achieves exact integration for any polynomial of degree $2n - 1$ or less using only n evaluation points, making it particularly advantageous in finite volume and spectral element methods where computational efficiency and accuracy are critical.

3.2.3 The mesh generation

Mesh generation is a crucial step in numerical simulations as it involves dividing a computational domain into smaller, discrete elements or cells to approximate the domain (Bern and Plassmann, 2000). This discrete representation is essential for solving PDEs using numerical methods such as the FEM, FVM, or FDM. The mesh provides the framework on which numerical solutions are computed, making its quality and accuracy fundamental to the success of a simulation. The process begins with accurately representing the geometry of the domain, ensuring that all boundaries and critical features are captured (Chawner et al., 2016). The mesh is composed of elements that can take various forms depending on the problem: lines for 1D simulations, triangles or quadrilaterals for 2D problems, and tetrahedra or hexahedra for 3D domains. The size and shape of these elements significantly influence the solution's accuracy and computational efficiency. Small elements provide higher resolution but increase computational cost, while large elements reduce resolution and may miss critical features of the solution.

Mesh quality is a vital consideration, as poorly designed meshes can lead to inaccuracies or instability in the numerical solution (Secco et al., 2021). Important factors include the aspect ratio of elements, which ideally should be close to one, and minimizing skewness or distortion in the mesh. Refinement is often necessary in regions with high gradients or complex phenomena, such as near boundaries or within shock waves. Adaptive meshing techniques

allow the mesh to evolve during the simulation, concentrating computational resources where they are most needed. The importance of mesh generation lies in its impact on the accuracy, efficiency, and stability of numerical simulations. A high-quality mesh ensures an accurate approximation of the domain, enabling better resolution of physical phenomena (Secco et al., 2021). It also balances computational cost by allowing coarse meshes in uniform regions and fine meshes in areas of interest. Numerical stability is another critical aspect, as poorly generated meshes can lead to convergence issues or unreliable solutions.

Mesh generation also facilitates the resolution of complex geometries, ensuring that intricate features are adequately represented in the simulation (Li et al., 2024). It can be tailored to the specific requirements of the problem, such as incorporating boundary-layer refinement for fluid dynamics problems. However, challenges remain, particularly for domains with sharp edges, holes, or irregular shapes. Balancing cost and accuracy is another challenge, as overly fine meshes increase computational expense, while overly coarse meshes compromise accuracy.

Various tools and techniques are employed to overcome these challenges. Manual mesh design is sometimes used for simple geometries, while automatic mesh generators, such as ANSYS Meshing, Gmsh, or HyperMesh, streamline the process for more complex domains (Liu, 2006). Adaptive mesh refinement (AMR) further enhances efficiency by dynamically refining the mesh based on error estimates or solution gradients. Hybrid meshes, which combine structured and unstructured elements, are also popular for leveraging the strengths of both approaches.

The research generates a computational mesh for the carotid artery model. The mesh divides the geometry into discrete elements, such as triangles or quadrilaterals, to facilitate the numerical calculations. The mesh quality and resolution are chosen based on Figure 1.3. The model equation for the research is designed considering the three regions indicated in Figure 1.4 and Figure 3.1 as follows:

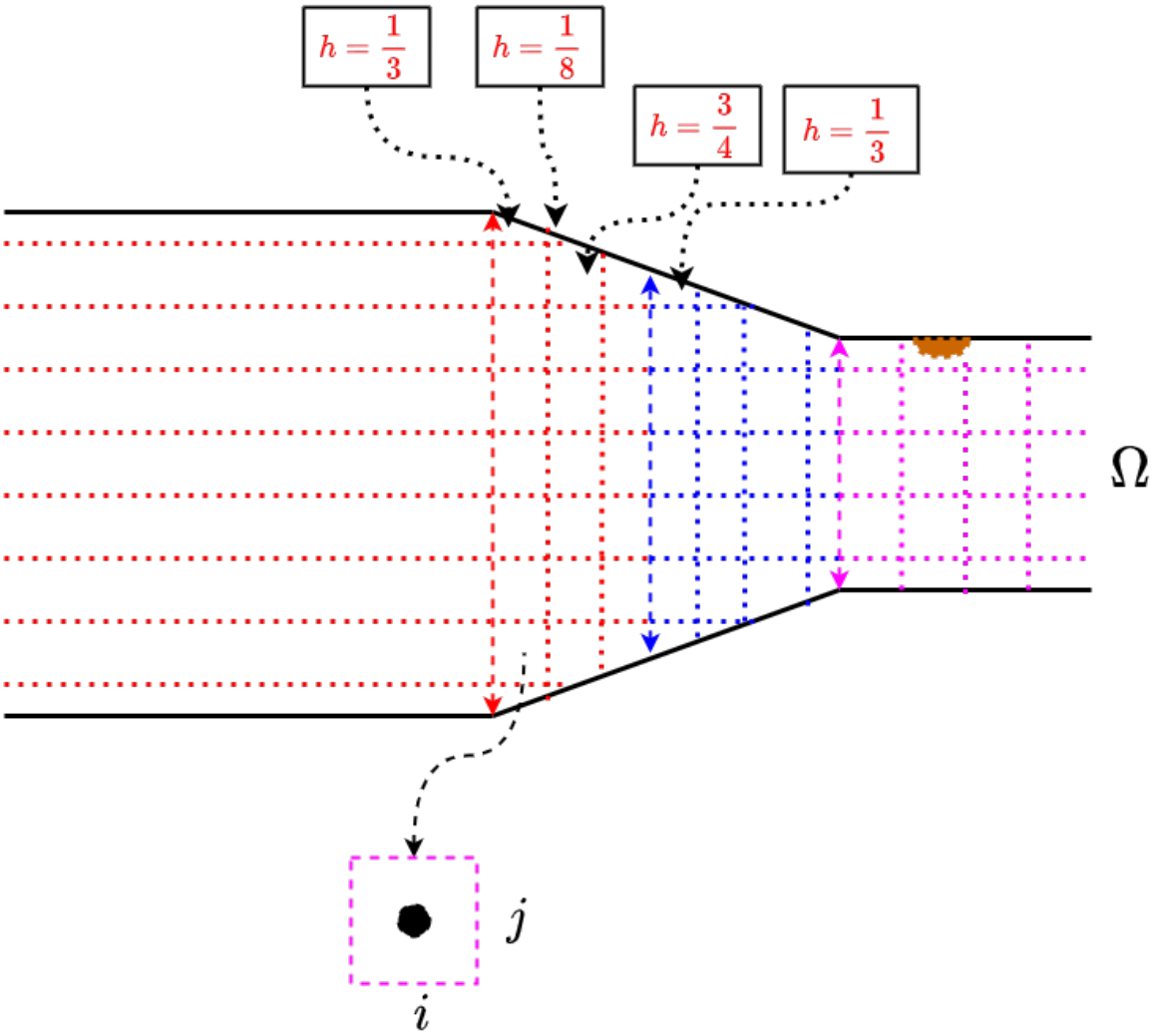

Figure 3.1: The mesh framework for discretizing the model diagram.

Source: Researcher, (2023).

The boundary conditions reflect physiological inlet pressure and no-slip arterial wall constraints, capturing the velocity profile realistically. Suppose $h = 1, \frac{1}{2}, \frac{1}{3}, \frac{1}{8}, \frac{3}{4}$ is the spatial discretization parameters. To apply the Gauss-Legendre quadrature in the discretized form based on finite volume method in order to find weights and nodes to approximate the integral, the formula for integrating function $f(r)$ over $[0, 1]$ is given by

$$\int_0^1 f(r)dr \approx \sum_{i=1}^{n} w_i.f\,(r_i) \tag{3.7}$$

where w_i is the weights and r_i are the nodes of the quadrature points. Assuming specific interval $[0, 1]$, then the transformation of $r = \frac{d}{2}\xi + \frac{d}{2}$, where d is the smallest diameter of a carotid artery and ξ is the unit of measurement of the diameter. Using the same analogy for Q Equation (1.27) yields

$$Q_{i,j}^{n+1} = \sum_{i=1}^{n} w_i \cdot \left[\frac{\pi r_{i,j}^4}{8\mu L} \left(1 - \frac{R_{i,j}^2}{r_{i,j}^2} \right) \left(P_{i,j}^{n+1} - \Delta P_{i,j}^{n+1} - \frac{8\mu L V_{i,j}^{n+1}}{r_{i,j}^2} \right) + W_{i,j}^{n+1} \left(r_{i,j}, t \right) \right] \tag{3.8}$$

where $r_{i,j}$ is the is the Gauss-Legendre quadrature point in the radial direction at the control volume (i, j). The subscripts i and j represent the indices in the spatial discretization, and the superscript $n + 1$ represents the time level. The weights w_i and the nodes ξ_i for Gauss-Legendre quadrature can be determined based on the number of quadrature points chosen. The governing equation for the research is given by

$$\begin{aligned} Q_{i,j}^{n+1} = \sum_{i=1}^{n} \Bigg[& \left(Q_{\left(1+\frac{1}{8},1\right)}^{n+1} + Q_{\left(1+\frac{1}{2},1\right)}^{n+1} + Q_{\left(1+\frac{3}{4},1\right)}^{n+1} + Q_{\left(1+\frac{1}{3},1\right)}^{n+1} \right) \\ & + \left(Q_{\left(1,1+\frac{1}{8}\right)}^{n+1} + Q_{\left(1,1+\frac{1}{2}\right)}^{n+1} + Q_{\left(1,1+\frac{3}{4}\right)}^{n+1} + Q_{\left(1,1+\frac{1}{3}\right)}^{n+1} \right) + Q_{(1,1)}^{n+1} \Bigg] \end{aligned} \tag{3.9}$$

Equation (3.9) represents an original modification of the classical Poiseuille equation by integrating drag loss terms and the Womersley function to reflect pulsatile, turbulent blood flow, particularly post-accident. Boundary conditions were selected to reflect no-slip conditions at the arterial wall and physiological pressure inputs based on known carotid artery data.

3.2.4 Non-dimensionalization

The variable parameters will be non-dimensionalized as follows: $\check{r} = \frac{R}{r_3}; \check{Q} = \frac{Q}{Q_0}$ where $Q_0 = \frac{\pi R^4}{8\mu L}; \check{P} = \frac{P}{\Delta P}$ with ΔP being the reference pressure; $\check{W} = \frac{W}{\frac{\pi R^4}{8\mu L}}$ with $\frac{\pi R^4}{8\mu L}$ being the reference term. The governing equations are subject to the following boundary conditions

$$Q(x,y,t) \geq 0; Q(x,y,0) = 0; Q(0,y,t) = 0; Q(x,0,t) = 0. \tag{3.10}$$

The governing equation in its non-dimensionalized form is given by:

$$\begin{aligned} \check{Q}_{i,j}^{n+1} = \sum_{i=1}^{n} \Bigg[& \left(\check{Q}_{\left(1+\frac{1}{8},1\right)}^{n+1} + \check{Q}_{\left(1+\frac{1}{2},1\right)}^{n+1} + \check{Q}_{\left(1+\frac{3}{4},1\right)}^{n+1} + \check{Q}_{\left(1+\frac{1}{3},1\right)}^{n+1} \right) \\ & + \left(\check{Q}_{\left(1,1+\frac{1}{8}\right)}^{n+1} + \check{Q}_{\left(1,1+\frac{1}{2}\right)}^{n+1} + \check{Q}_{\left(1,1+\frac{3}{4}\right)}^{n+1} + \check{Q}_{\left(1,1+\frac{1}{3}\right)}^{n+1} \right) \\ & + \check{Q}_{(1,1)}^{n+1} \Bigg]. \end{aligned} \tag{3.11}$$

The governing equations are subject to the following boundary conditions:

$$\check{Q}(x,y,t) \geq 0, \quad \check{Q}(x,y,0) = 0, \quad \check{Q}(0,y,t) = 0, \quad \check{Q}(x,0,t) = 0. \tag{3.12}$$

CHAPTER FOUR

RESULTS AND DISCUSSION

4.1 Introduction

The study developed a novel Poiseuille-based mathematical model for blood flow in the pulsatile carotid artery in Equation (3.11). The study investigated the impact of geometric interruption of blood flow on carotid artery for a novel Poiseuille-based mathematical equation. The study investigated the impact of vascular stress and pulsatility on blood flow on carotid artery for a novel Poiseuille-based mathematical equation.

4.2 Simulation

4.2.1 Parameter Estimation and Fitting

The novel Poiseuille-based mathematical model for blood flow in the pulsatile carotid artery presented in Equation (3.11) was solved numerically via Matlab based on the parameter values presented in Table 4.1. The simulation was then run for different total simulation time from $t = 5 \rightarrow 100$ in order to evaluate the study objectives. The simulation time interval $[5s, 100s]$ was selected to capture initial transients and steady-state behavior of blood flow post-geometry interruption. All time values are expressed in seconds (s), and velocity in meters per second (m/s).

Table 4.1: Parameter values

Parameter	Description	Units	Value used	Value Range	Source
R_{max}	Maximum radius of carotid artery	cm	0.265	0.305 ± 0.04	(Kpuduwei et al., 2022)
P	pressure difference between the two ends of the artery	mm Hg	-1.333	-1.333 ± 6.548	(Soleimani et al., 2017)
ΔP	pressure drop due to the reduced arterial diameter	mm Hg	80	75-85	(Soueidan et al., 2010)
f	drag coefficient	%	0.61	0.58-0.64	(Seymour et al., 2020)
L	Length of the carotid artery	cm	21.65	$22.2 \pm 2.2 - 20.8 \pm 1.9$	(Choudhry et al., 2016)
ρ	density of blood	kg/m^3	1060	-	(Vitello et al., 2015)
V	velocity of blood	cm/sec	-	30-40	(Lee, 2014)
μ	dynamic viscosity of blood	cP	4.5	3.5 -5.5	(Nader et al., 2019)

4.2.2 Geometric Interruption of Blood flow on Carotid artery via a novel Poiseuille-based model

In order to evaluate the interruption of geometry on blood flow, the proposed Poiseuille model for blood flow in the pulsatile carotid artery presented in Equation (1.27) is solved and simulated graphically. The results are presented in Figure 4.1.

Figure 4.1 shows four plots, where the first plot indicates a 3D plot of time against radius and Q (blood flow rate). The second figure indicates a 3D time plot against radius and U (velocity of blood). The third plot shows radius against Q, and the fourth is a plot of time against velocity, U and blood flow rate, Q. The t plot against R and Q indicates that Q reduces as the radius increases. This is because the flow rate through a vessel depends not only on its radius but also on the pressure difference across the artery, the blood's viscosity, and the artery's length. In turbulent flow conditions, as in this case, the flow is characterized by chaotic and irregular fluid motion, and the relationship between flow rate and radius becomes more complex. Turbulent flow can occur at higher flow velocities or in artery with irregular geometries or high Reynolds numbers. In such cases, an increase in radius may not necessarily result in a proportional increase in flow rate due to the turbulent nature of the flow. In the case of this research, the flow rate reduces as the radius increases due to an increase in vascular stress. It is also expected that as velocity increases, so does the flow rate.

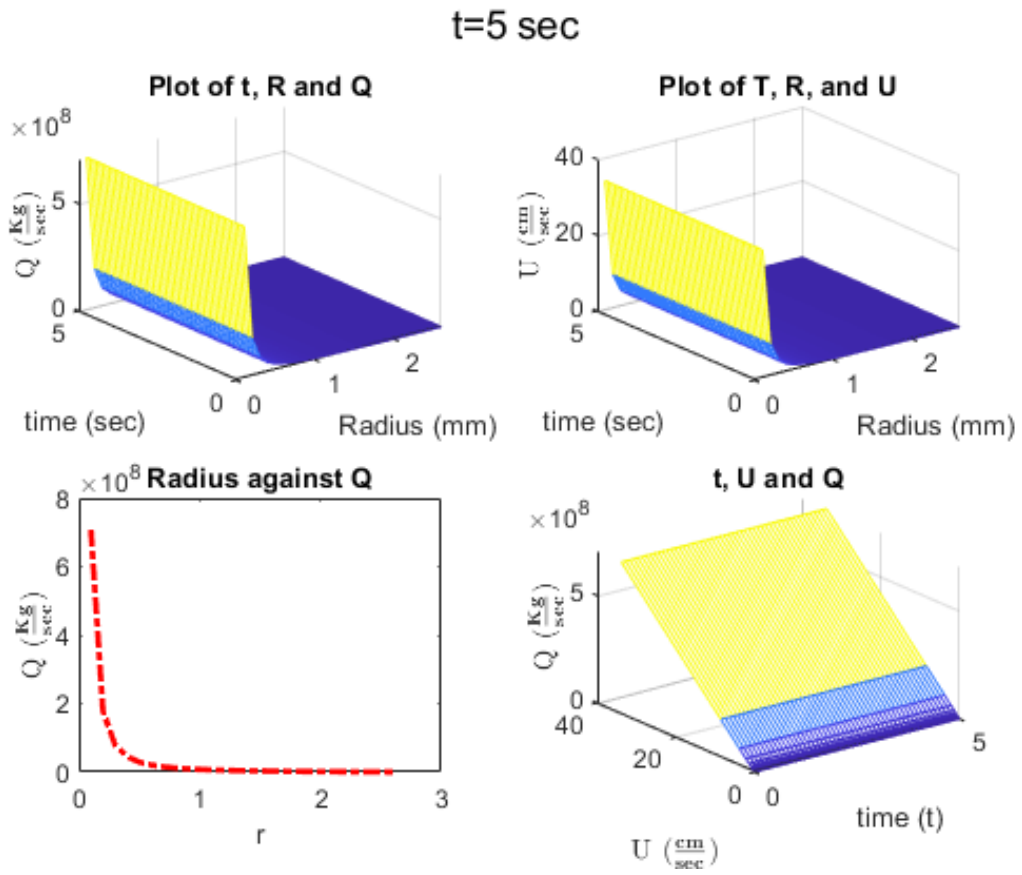

Figure 4.1: The results for simulation time of 5 sec.

4.2.3 Vascular stress

The third objective was the effect of vascular stress and pulsatility on blood flow on carotid artery for a novel Poiseuille-based mathematical. The results is presented in Figure 4.2.

Figure 4.2 indicates that vascular stress $W(r,t)$ increases as the radius of the carotid artery reduces. Vascular stress refers to the force per unit area applied to the walls of blood vessels. The stress experienced by the artery walls is influenced by various factors, including blood pressure, flow rate, and the geometry of the blood vessel, represented by its radius (r). According to the law of Hagen-Poiseuille, the stress or pressure drop (ΔP) across a cylindrical vessel is directly proportional to the flow rate (Q), the viscosity of blood (μ) and inversely proportional to the fourth power of the radius of the artery (r). This relationship is expressed as $\Delta P = \frac{8\mu LQ}{\pi r^4}$ based on Equation (1.27). Therefore, as the radius of the artery reduces, the

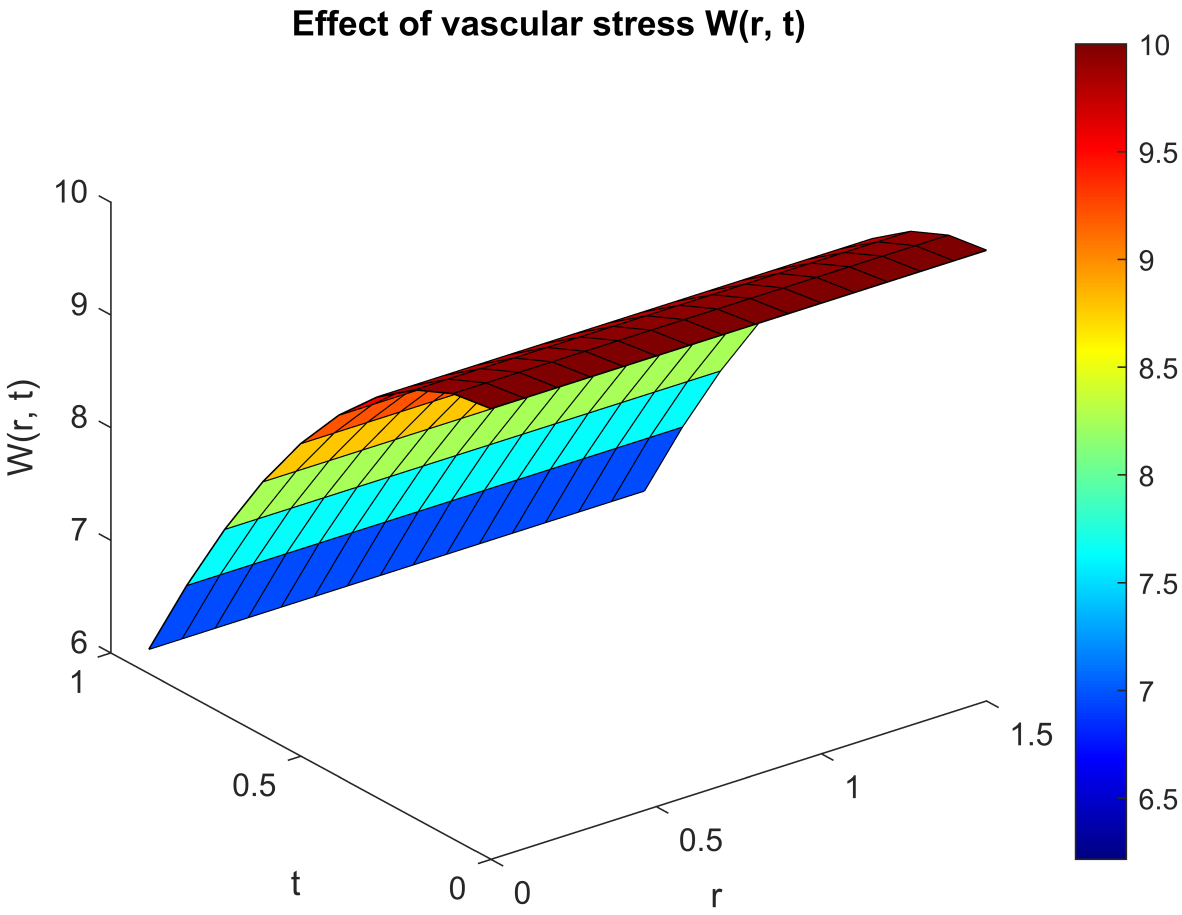

Figure 4.2: The impact of vascular stress and pulsatility on blood flow on carotid artery.

denominator (r^4) decreases, leading to an increase in the pressure drop (ΔP) and, consequently, an increase in vascular stress $W(r,t)$. So, as the radius of the carotid artery reduces, the stress experienced by its walls increases.

4.3 Discussion

The general observation in the study (see Figure 4.3) is that when $r = 1.5mm$ and $t = 0.9sec$, the flow rate, Q becomes zero. This explains why in case of accidents and the victims get injuries on the neck they succumb during the accident. Notably, the empirical velocity according to Lee (2014) is $V = 30-40cm/sec$. The simulated velocity based on Equation 1.27 is $33.8419cm/sec$, which is within the range given in literature. Such observation indicates the reliability of the study results.

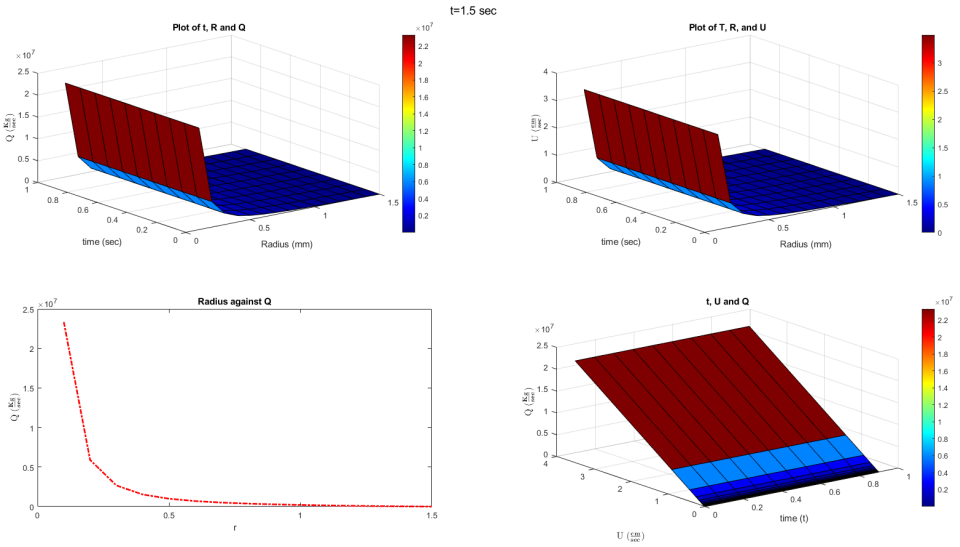

Figure 4.3: The results for simulation time of 1.5 sec.

4.3.1 Geometric Interruption of Blood flow on Carotid artery via a novel Poiseuille-based model

The simulation results of pulsatile blood flow in the carotid artery using a Poiseuille-based model are presented in Figure 4.1. This section interprets the observed hemodynamic behaviors under turbulent conditions, focusing on the influence of arterial geometry on flow rate Q, velocity U, and radius R, and evaluates how the results align with theoretical expectations in vascular fluid mechanics.

The first plot in Figure 4.1 depicts a three-dimensional surface of flow rate Q as a function of radius and time. Contrary to the classical Poiseuille expectation that flow rate increases with radius in laminar conditions—according to the proportionality $Q \propto R^4$—the present results show a decrease in Q with increasing radius under turbulent conditions. This deviation can be attributed to the onset of geometric disturbances and secondary flow structures that dominate in post-stenotic or bifurcated regions. As reported by Hameed et al. (2023), turbulent flows exhibit chaotic velocity fluctuations and eddy formations, which increase energy losses and wall stress, thereby disrupting the monotonic increase in flow rate predicted by laminar theory.

The second plot further confirms this trend by illustrating how the reduction in flow rate persists over time as the radius increases. This non-linear behavior is consistent with theoretical models of disturbed flow in arterial systems, where alterations in vessel geometry—such as dilation, curvature, or post-stenotic expansions—can induce localized turbulence and flow separation. Singh and Singh (2022) noted that such geometrical deviations significantly alter flow field symmetry and resistance, especially beyond bifurcation points, leading to reduced effective perfusion.

The third plot offers a more direct analysis of the relationship between radius and flow rate Q, once again revealing an inverse correlation under turbulent conditions. While classical laminar theory would predict increased flow with wider luminal diameter, the results here suggest that under disrupted flow regimes, enlarged radii may introduce adverse pressure gradients and backflow zones. These contribute to increased effective resistance and a net reduction in forward flow, particularly in pathological segments such as aneurysmal expansions or irregular post-traumatic geometries. This observation aligns with findings by Hameed et al. (2023), who reported similar inverse trends in stenosed models exhibiting turbulent backflow and elevated wall shear stress (WSS).

The fourth plot explores the relationship between time, velocity U, and flow rate Q. A direct correlation is observed between U and Q, which is in agreement with the fundamental continuity and momentum principles of fluid mechanics, where increased axial velocity enhances volumetric throughput. This result is consistent with prior literature, such as Fusi and Farina (2020), who emphasized that in pulsatile and disturbed flow regimes, localized increases in velocity are required to maintain perfusion despite geometric resistance or hematocrit-related viscosity changes.

The simulation results exhibit good agreement with established theoretical and empirical findings. Studies by Hameed et al. (2023) and Singh and Singh (2022) confirm that arterial stenosis and bifurcations significantly influence flow patterns by introducing turbulence, reverse flow, and high shear regions—features that are replicated in the current model. Fur-

thermore, works by Dhange et al. (2022b) and Sarifuddin (2022) have shown that vascular resistance increases non-linearly with stenosis severity, leading to diminished flow rates—a phenomenon also observed in this simulation through elevated vascular stress and declining Q with increasing radius.

These findings reinforce the notion that the classical Poiseuille model, while effective under idealized laminar conditions, requires modification to capture the complex dynamics of blood flow in geometrically perturbed and turbulent arterial regions. The model's deviations under these conditions underscore the necessity for incorporating turbulent correction factors and non-Newtonian effects in future CFD-based hemodynamic studies.

4.3.2 Vascular stress

The third objective of this study was to examine the effects of vascular stress and pulsatility on blood flow in the carotid artery using a novel Poiseuille-based mathematical model. The results, presented in Figure 4.2, provide important insights into the relationship between vascular stress, arterial radius, and blood flow, with implications for understanding cardiovascular dynamics and potential treatments for arterial diseases.

Figure 4.2 illustrates the increase in vascular stress $W(r,t)$ as the radius of the carotid artery decreases. Vascular stress is defined as the force per unit area exerted by the flowing blood on the vessel wall. The governing relationship for this stress is derived from Hagen–Poiseuille's law, which relates the pressure drop (ΔP) across a cylindrical vessel to the radius of the vessel:

$$\Delta P = \frac{8\mu LQ}{\pi r^4}, \tag{4.1}$$

where r is the radius of the artery, Q is the volumetric flow rate, μ is the dynamic viscosity of blood, and L is the length of the vessel. As the radius decreases, the denominator r^4 diminishes sharply, leading to a pronounced increase in pressure drop ΔP. This increase translates directly into heightened vascular stress $W(r,t)$, a phenomenon frequently associated with

arterial narrowing, as seen in stenotic or atherosclerotic arteries.

The finding that vascular stress increases with decreasing arterial radius aligns with established principles of fluid dynamics under both laminar and turbulent flow regimes. In arteries such as the carotid, which are particularly susceptible to atherosclerotic narrowing, reductions in vessel diameter cause a significant rise in wall shear stress (WSS) and overall vascular load. Elevated WSS has been identified as a major contributor to endothelial dysfunction and plaque instability, which can lead to progressive vascular disease.

According to Hameed et al. (2023), high wall shear stress and irregular flow patterns are characteristic features of diseased carotid arteries. Their research demonstrated that stenotic arteries exhibit fluctuating velocity and pressure fields, especially at bifurcation points where disturbed flow prevails. The present findings are consistent with those observations, indicating that as arterial radius decreases, vascular stress intensifies, potentially accelerating disease progression through mechanical irritation and inflammatory response at the vessel wall.

Similarly, Dhange et al. (2022b) observed that narrowing arteries experience increased surface shear stress and hydraulic resistance, emphasizing that the severity of stenosis directly correlates with elevated wall stress. This relationship mirrors the results shown in Figure 4.2, where the increase in vascular stress accompanies reductions in radius. Severe narrowing can therefore precipitate complications such as arterial rupture or thrombosis due to localized mechanical overload.

The pulsatile nature of blood flow further amplifies these stress effects. Blood flow in large arteries like the carotid is inherently pulsatile, driven by the rhythmic pumping of the heart. Fusi and Farina (2020) analyzed Poiseuille flow stability under varying red blood cell (RBC) concentrations and reported that RBC aggregation near the vessel wall contributes to flow instability, thereby increasing wall stress in regions of geometric constriction. In the present model, pulsatility magnifies the stress variations observed in narrowed segments. During systole, when ventricular contraction increases arterial pressure and velocity, the shear force on the vessel wall peaks, particularly in constricted regions. As the radius decreases, these pul-

satile forces become more intense, resulting in periodic mechanical loading that can weaken the arterial wall over time, consistent with findings by Singh and Singh (2022) on bifurcation-induced stress concentrations.

The current simulation outcomes also align closely with earlier computational studies. Fojas and De Leon (2013) developed a two-dimensional model of carotid artery bifurcation and found that regions of high wall shear stress correspond to arterial narrowing or branching zones. Their results demonstrated that geometric alterations, such as those caused by stenosis, produce significant increases in vascular stress and turbulence, an observation corroborated by the present findings. Similarly, Sarifuddin (2022) investigated the hemodynamic impact of arterial stenosis and reported that as the degree of narrowing increases, wall shear stress and vascular stress both intensify. The inverse relationship between radius and stress in this study supports these conclusions, underscoring how geometrical constriction drives adverse hemodynamic conditions.

The observed increase in vascular stress with decreasing arterial radius has notable clinical implications. Elevated wall shear stress is a well-documented factor in the initiation and progression of atherosclerosis and other vascular disorders. The results of this study suggest that mitigating arterial narrowing, through surgical interventions such as stenting or angioplasty, or via pharmacological management of vascular tone, can significantly reduce vascular stress and improve arterial health. Hameed et al. (2023) emphasized the importance of maintaining laminar flow and minimizing stress fluctuations in post-stenotic or stented arteries. Restoring physiological flow conditions and reducing stress oscillations may therefore decrease the risk of arterial wall damage, enhance vascular recovery, and improve patient outcomes.

The modeled relationship between vascular stress, arterial radius, and pulsatile dynamics provides a mechanistic explanation for the onset and progression of vascular disease in the carotid artery. The findings reinforce the need for advanced hemodynamic models that integrate pulsatility, turbulence, and non-Newtonian blood properties to more accurately predict stress distribution and guide clinical interventions in arterial pathologies.

CHAPTER FIVE

SUMMARY, CONCLUSION AND RECOMMENDATIONS

5.1 Summary

This study applied the Poiseuille equation to model blood flow in the carotid artery due to its relevance in describing laminar flow in cylindrical vessels. While suitable for large and medium-sized arteries under steady, incompressible flow conditions, its limitations became evident in turbulent and pulsatile regimes, especially in stenosed or geometrically interrupted arteries. The study addressed key research gaps concerning vascular shear stress, pulsatile effects, and the influence of carotid artery geometry on flow dynamics.

5.1.1 Geometric Interruption and Flow Dynamics in the Carotid Artery

Simulations using the Poiseuille-based model revealed that geometric disturbances, such as bifurcations and stenosis, led to a decrease in flow rate Q and an increase in vascular stress, particularly under turbulent conditions. This non-linear behavior, where flow rate inversely correlated with radius R, aligns with existing literature on stenosed arteries (Hameed et al., 2023; Singh and Singh, 2022). Additionally, a direct relationship between velocity U and flow rate was observed, consistent with established fluid dynamics (Fusi and Farina, 2020). These findings highlight the limitations of the Poiseuille model in non-laminar flow scenarios and underscore the need for enhanced modeling approaches in geometrically complex arteries.

5.1.2 Vascular Stress and Pulsatility

The study also evaluated the impact of vascular stress $W(r,t)$ and pulsatile flow. Results showed that as the artery radius r decreased, vascular stress significantly increased, consistent with Hagen–Poiseuille's law. This increase was further amplified during systolic phases due to pulsatile blood flow. Such elevated stress levels are associated with vascular complications, including stenosis, and have been confirmed in previous computational and clinical studies (Dhange et al., 2022b; Fojas and De Leon, 2013; Singh and Singh, 2022). The findings underscore the model's limitations in capturing the full spectrum of hemodynamic phenomena in real physiological conditions and reinforce the importance of accounting for pulsatility and turbulence in future models.

5.2 Conclusion

This research achieved its objectives by developing and evaluating a Poiseuille-based model for blood flow in the carotid artery. The study investigated the effects of geometric interruptions, vascular stress, and pulsatility, revealing that while the model performs adequately under laminar conditions, it lacks robustness in turbulent and pulsatile regimes. The results affirm the necessity for more comprehensive models that incorporate arterial geometry, time-dependent behavior, and shear-driven effects to accurately simulate carotid artery hemodynamics.

5.2.1 Key Findings

- Geometric interruptions, such as stenosis or bifurcations, were shown to reduce flow rate Q and increase vascular stress under turbulent flow conditions.
- A non-linear inverse relationship between radius and flow rate was observed, diverging from classical Poiseuille predictions under non-laminar regimes.
- Pulsatility significantly influenced stress distribution, particularly during systolic phases,

further elevating wall shear stress $W(r,t)$ in narrowed segments.

- The study highlighted the limitations of classical models in accurately capturing complex arterial flow and emphasized the need for models that incorporate pulsatile and turbulent effects.

5.3 Recommendations

5.3.1 Future Research Directions

(i) Develop advanced computational models that extend Poiseuille's framework to include turbulence modeling and pulsatile flow characteristics.

(ii) Investigate the role of non-Newtonian blood properties under varying shear conditions to improve the accuracy of vascular stress predictions.

(iii) Incorporate patient-specific arterial geometries and physiological data to support personalized diagnostics and treatment planning for vascular diseases.

5.3.2 Policy and Clinical Recommendations

(i) Encourage integration of advanced blood flow modeling tools in diagnostic workflows to improve early detection of vascular pathologies such as stenosis.

(ii) Support the design and development of stents and pharmaceutical interventions aimed at minimizing vascular stress in narrowed arteries.

(iii) Mandate the adoption of computational modeling in clinical practice to improve surgical planning and risk assessment for patients with arterial abnormalities.

REFERENCES

Alexy, T., Detterich, J., Connes, P., Toth, K., Nader, E., Kenyeres, P., Arriola-Montenegro, J., Ulker, P., and Simmonds, M. J. (2022). Physical properties of blood and their relationship to clinical conditions. *Frontiers in Physiology*, 13:906768.

Ashoor, M., Khorshidi, A., Pirouzi, A., Abdollahi, A., Mohsenzadeh, M., and Barzi, S. M. Z. (2021). Estimation of reynolds number on microvasculature capillary bed using diffusion and perfusion mri: the theoretical and experimental investigations. *The European Physical Journal Plus*, 136(2):152.

Avgerinos, N. A. and Neofytou, P. (2019). Mathematical modelling and simulation of atherosclerosis formation and progress: a review. *Annals of Biomedical Engineering*, 47:1764–1785.

Babich, D. B. W. C. (2021). Car accidents can cause deadly carotid artery aneurysms. `https://www.dbbwc.com/blog/2021/october/car-accidents-can-cause-deadly-carotid-artery-an/`.

Bern, M. W. and Plassmann, P. E. (2000). Mesh generation. *Handbook of computational geometry*, 38.

Bertaglia, G., Caleffi, V., and Valiani, A. (2020). Modeling blood flow in viscoelastic vessels: the 1d augmented fluid–structure interaction system. *Computer Methods in Applied Mechanics and Engineering*, 360:112772.

Blokhin, A. and Tkachev, D. (2020). Stability of the poiseuille-type flow for a mhd model of an incompressible polymeric fluid. *European Journal of Mechanics-B/Fluids*, 80:112–121.

Campinho, P., Vilfan, A., and Vermot, J. (2020). Blood flow forces in shaping the vascular system: a focus on endothelial cell behavior. *Frontiers in physiology*, 11:552.

Carvalho, V., Pinho, D., Lima, R. A., Teixeira, J. C., and Teixeira, S. (2021). Blood flow modeling in coronary arteries: A review. *Fluids*, 6(2):53.

Chawner, J. R., Dannenhoffer, J., and Taylor, N. J. (2016). Geometry, mesh generation, and the cfd 2030 vision. In *46th AIAA Fluid Dynamics Conference*, page 3485.

Chen, Z., Zhu, L.-T., and Luo, Z.-H. (2023). Characterizing flow and transport in biological vascular systems: A review from physiological and chemical engineering perspectives. *Industrial & Engineering Chemistry Research*, 63(1):4–36.

Choudhry, F. A., Grantham, J. T., Rai, A. T., and Hogg, J. P. (2016). Vascular geometry of the extracranial carotid arteries: an analysis of length, diameter, and tortuosity. *Journal of neurointerventional surgery*, 8(5):536–540.

Claassen, J. A., Thijssen, D. H., Panerai, R. B., and Faraci, F. M. (2021). Regulation of cerebral blood flow in humans: physiology and clinical implications of autoregulation. *Physiological reviews*, 101(4):1487–1559.

Clevenger, A. C., Kilbaugh, T., and Margulies, S. S. (2015). Carotid artery blood flow decreases after rapid head rotation in piglets. *Journal of neurotrauma*, 32(2):120–126.

Csippa, B. (2023). Hemodynamics of arterial malformations: Intracranial aneurysms and coronary artery disease. *National Library of Medicine*.

Dhange, M., Sankad, G., and Bhujakkanavar, U. (2022a). Modeling of blood flow with stenosis and dilatation. *Mathematics and Mechanics of Complex Systems*, 10(2):155–169.

Dhange, M., Sankad, G., Safdar, R., Jamshed, W., Eid, M. R., Bhujakkanavar, U., Gouadria, S., and Chouikh, R. (2022b). A mathematical model of blood flow in a stenosed artery with post-stenotic dilatation and a forced field. *Plos one*, 17(7):e0266727.

Dutra, R., Zinani, F., Rocha, L., and Biserni, C. (2021). Effect of non-newtonian fluid rheology on an arterial bypass graft: A numerical investigation guided by constructal design. *Computer Methods and Programs in Biomedicine*, 201:105944.

Ellis, J. A. and Joshi, S. (2025). Cerebral and spinal cord blood flow. In *Cottrell & Patel's Neuroanesthesia*, pages 22–66. Elsevier.

Farkhutdinov, T., Gay-Balmaz, F., and Putkaradze, V. (2020). Geometric variational approach to the dynamics of porous medium, filled with incompressible fluid. *Acta Mechanica*, 231(9):3897–3924.

Fojas, J. J. R. and De Leon, R. L. (2013). Carotid artery modeling using the navier-stokes equations for an incompressible, newtonian and axisymmetric flow. *APCBEE procedia*, 7:86–92.

Freidoonimehr, N., Arjomandi, M., Sedaghatizadeh, N., Chin, R., and Zander, A. (2020). Transitional turbulent flow in a stenosed coronary artery with a physiological pulsatile flow. *International Journal for Numerical Methods in Biomedical Engineering*, 36(7):e3347.

Fusi, L. and Farina, A. (2020). Linear stability analysis of blood flow in small vessels. *Applications in Engineering Science*, 1(100002):100002.

Gamal, M., Kotb, M., Naguib, A., and Elsherbiny, K. (2021). Numerical investigations of micro bubble drag reduction effect for container ships. *Marine Systems & Ocean Technology*, 16:199–212.

Gazzola, F. and Sperone, G. (2020). Steady navier–stokes equations in planar domains with obstacle and explicit bounds for unique solvability. *Archive for Rational Mechanics and Analysis*, 238(3):1283–1347.

Ghitti, B., Toro, E. F., and Müller, L. O. (2022). Nonlinear lumped-parameter models for blood flow simulations in networks of vessels. *ESAIM: Mathematical Modelling and Numerical Analysis*, 56(5):1579–1627.

Hameed, M. S., Shah, A. A., Khan, M. I., Ali, A., Hussain, I., and Bukhari, M. D. (2023). Comparison of blood flow analysis in stenosed and stented carotid artery bifurcation models. *Cogent Engineering*, 10(1):2158624.

Heck, D. and Jost, A. (2021). Carotid stenosis, stroke, and carotid artery revascularization. *Progress in Cardiovascular Diseases*, 65:49–54.

Holmes, D. W. and Pivonka, P. (2021). Novel pressure inlet and outlet boundary conditions for smoothed particle hydrodynamics, applied to real problems in porous media flow. *Journal of Computational Physics*, 429:110029.

Johansson, F. and Mezzarobba, M. (2018). Fast and rigorous arbitrary-precision computation of gauss–legendre quadrature nodes and weights. *SIAM Journal on Scientific Computing*, 40(6):C726–C747.

Kannojiya, V., Das, A. K., and Das, P. K. (2020). Simulation of blood as fluid: A review from rheological aspects. *IEEE Reviews in Biomedical Engineering*, 14:327–341.

Karthik, A., Kumar, P. P., and Radhika, T. (2022). A mathematical model for blood flow accounting for the hematological disorders. *Computational and Mathematical Biophysics*, 10(1):184–198.

Khalid, A., Othman, Z., and Shafee, C. M. (2021). A review of mathematical modelling of blood flow in human circulatory system. In *Journal of Physics: Conference Series*, volume 1988, page 012010. IOP Publishing.

Kim, J.-H. (2022). Heart and circulatory system. In *Recent Advancements in Microbial Diversity*, pages 229–254. Elsevier.

Kollmann, W. (2024). Navier-stokes equations. In *Navier-Stokes Turbulence: Theory and Analysis*, pages 19–57. Springer.

Kpuduwei, S., Kiridi, E., Fawehinmi, H., and Oladipo, G. (2022). Reference luminal diameters of the carotid arteries among healthy nigerian adults. *Folia Morphologica*, 81(3):579–583.

Kumar, J. P., Sadique, M., and Shah, S. R. (2022). Mathematical study of blood flow through blood vessels under diseased condition. *International Journal of Multidisciplinary Research and Development*, 9(6):31–44.

Lee, W. (2014). General principles of carotid doppler ultrasonography. *Ultrasonography*, 33(1):11.

Li, X., Yang, M., Bi, L., Xu, R., Luo, C., Yuan, S., Yuan, X., and Tang, Z. (2024). An efficient cartesian mesh generation strategy for complex geometries. *Computer Methods in Applied Mechanics and Engineering*, 418:116564.

Li, Y., Mu, J., Xiong, C., Sun, Z., and Jin, C. (2021). Effect of visco-plastic and shear-thickening/thinning characteristics on non-newtonian flow through a pipe bend. *Physics of Fluids*, 33(3).

Liu, H. (2006). 3-d mesh generation for finite-element modelling of complex natural structures. *eScholarship for McGill University*.

Liu, J., Lan, I. S., and Marsden, A. L. (2021). Mathematical modeling of the vascular system. *arXiv preprint arXiv:2102.11064*.

Lopes, D., Puga, H., Teixeira, J., and Lima, R. (2020). Blood flow simulations in patient-specific geometries of the carotid artery: A systematic review. *Journal of Biomechanics*, 111:110019.

Mimeau, C. and Mortazavi, I. (2021). A review of vortex methods and their applications: From creation to recent advances. *Fluids*, 6(2):68.

Montorfano, L., Sarkissyan, M., Wolfers, M., Rodríguez, F., Pla, F., and Montorfano, M. (2020). Pocus and pocdus: essential tools for the evaluation and management of carotid artery pseudoaneurysms after a gunshot wound. *The Ultrasound Journal*, 12(1):1–6.

Moreles, M. A., Peña, J., Botello, S., and Iturriaga, R. (2013). On modeling flow in fractal media form fractional continuum mechanics and fractal geometry. *Transport in porous media*, 99:161–174.

Myneni, M. and Rajagopal, K. (2022). Constitutive modeling of the mechanical response of arterial tissues. *Applications in Engineering Science*, 11:100111.

Nader, E., Skinner, S., Romana, M., Fort, R., Lemonne, N., Guillot, N., Gauthier, A., Antoine-Jonville, S., Renoux, C., Hardy-Dessources, M.-D., et al. (2019). Blood rheology: key parameters, impact on blood flow, role in sickle cell disease and effects of exercise. *Frontiers in physiology*, 10:1329.

Nichols, W. (2022). Nature of flow of a liquid. In *McDonald's Blood Flow in Arteries*, pages 25–67. CRC Press.

Owais, M., Usmani, A. Y., and Muralidhar, K. (2023). Effect of a bend on vortex formation and evolution in a three-dimensional stenosed geometry during pulsatile flow. *Physics of Fluids*, 35(3).

Pisano, A. and Pisano, A. (2021). From tubes and catheters to the basis of hemodynamics: Viscosity and hagen–poiseuille equation. *Physics for Anesthesiologists and Intensivists: From Daily Life to Clinical Practice*, pages 89–98.

Rao, A. R. and Mishra, M. (2004). Peristaltic transport of a power-law fluid in a porous tube. *Journal of Non-Newtonian Fluid Mechanics*, 121(2-3):163–174.

Rougier, V., Cellier, J., Gomina, M., and Bréard, J. (2021). Slip transition in dynamic wetting for a generalized navier boundary condition. *Journal of Colloid and Interface Science*, 583:448–458.

Roy, A. K. and Bég, O. A. (2021). Mathematical modelling of unsteady solute dispersion in two-fluid (micropolar-newtonian) blood flow with bulk reaction. *International Communications in Heat and Mass Transfer*, 122:105169.

Saktioto, S., Defrianto, D., Thoibah, A., Soerbakti, Y., Syahputra, R. F., Syamsudhuha, S., Irawan, D., Hairi, H., Okfalisa, O., and Amelia, R. (2023). Simplified kinetic model of

heart pressure for human dynamical blood flow. *Indonesian Journal of Electrical Engineering and Informatics (IJEEI)*, 11(3):870–882.

Sarifuddin (2022). CFD modelling of casson fluid flow and mass transport through atherosclerotic vessels. *Differ. Equ. Dyn. Syst.*, 30(2):253–269.

Secco, N. R., Kenway, G. K., He, P., Mader, C., and Martins, J. R. (2021). Efficient mesh generation and deformation for aerodynamic shape optimization. *AIAA Journal*, 59(4):1151–1168.

Sedaghat, S., Van Sloten, T. T., Laurent, S., London, G. M., Pannier, B., Kavousi, M., Mattace-Raso, F., Franco, O. H., Boutouyrie, P., Ikram, M. A., et al. (2018). Common carotid artery diameter and risk of cardiovascular events and mortality: pooled analyses of four cohort studies. *Hypertension*, 72(1):85–92.

Seymour, R. S., Hu, Q., and Snelling, E. P. (2020). Blood flow rate and wall shear stress in seven major cephalic arteries of humans. *Journal of Anatomy*, 236(3):522–530.

Shahzad, H., Wang, X., Ghaffari, A., Iqbal, K., Hafeez, M. B., Krawczuk, M., and Wojnicz, W. (2022). Fluid structure interaction study of non-newtonian casson fluid in a bifurcated channel having stenosis with elastic walls. *Scientific Reports*, 12(1):12219.

Siddqi, Z. F. (2024). Computational fluid dynamics: Modeling and analysis of blood flow in arteries. In *Motion Analysis of Biological Systems: Advanced Theoretical and Computational Concepts*, pages 89–121. Springer.

Singh, D. and Singh, S. (2022). Mathematical modelling of an incompressible, newtonian blood flow for the carotid artery. In *International workshop of Mathematical Modelling, Applied Analysis and Computation*, pages 259–272. Springer.

Skytioti, M., Elstad, M., and Søvik, S. (2019). Internal carotid artery blood flow response to anesthesia, pneumoperitoneum, and head-up tilt during laparoscopic cholecystectomy. *Anesthesiology*, 131(3):512–520.

Soleimani, E., Mokhtari-Dizaji, M., Fatouraee, N., and Saberi, H. (2017). Assessing the blood pressure waveform of the carotid artery using an ultrasound image processing method. *Ultrasonography*, 36(2):144.

Soueidan, K., Chen, S., Dajani, H. R., Bolic, M., and Groza, V. (2010). The effect of blood pressure variability on the estimation of the systolic and diastolic pressures. In *2010 IEEE International Workshop on Medical Measurements and Applications*, pages 14–18. IEEE.

Spencer, H. (2020). *The Principles of Biology: Volume 1*. Outlook Verlag.

Tigges, T. (2023). *Non-invasive Detection of Hypovolemia by Multimodal Body Sensor Network*. PhD thesis, Technische Universitaet Berlin (Germany).

Trejo-Soto, C. and Hernández-Machado, A. (2022). Normalization of blood viscosity according to the hematocrit and the shear rate. *Micromachines*, 13(3):357.

Van Hoecke, L., Boeye, D., Gonzalez-Quiroga, A., Patience, G. S., and Perreault, P. (2023). Experimental methods in chemical engineering: Computational fluid dynamics/finite volume method—cfd/fvm. *The Canadian Journal of Chemical Engineering*, 101(2):545–561.

Vitello, D. J., Ripper, R. M., Fettiplace, M. R., Weinberg, G. L., and Vitello, J. M. (2015). Blood density is nearly equal to water density: a validation study of the gravimetric method of measuring intraoperative blood loss. *Journal of veterinary medicine*, 2015.

Wajihah, S. A. and Sankar, D. (2023). A review on non-newtonian fluid models for multilayered blood rheology in constricted arteries. *Archive of Applied Mechanics*, 93(5):1771–1796.

Wang, J. (2022). *Multiscale modelling of haemorrhagic transformation after ischaemic stroke*. PhD thesis, University of Oxford.

Wang, S. (2023). Physiology of extracorporeal life support. In *Extracorporeal life support*, pages 1–20. Springer.

Wang, X., Qiao, Y., Qi, H., and Xu, H. (2022). Numerical study of pulsatile non-newtonian blood flow and heat transfer in small vessels under a magnetic field. *International Communications in Heat and Mass Transfer*, 133:105930.

Wedel, J., Štrakl, M., Ravnik, J., Steinmann, P., and Hriberšek, M. (2022). A specific slip length model for the maxwell slip boundary conditions in the navier–stokes solution of flow around a microparticle in the no-slip and slip flow regimes. *Theoretical and Computational Fluid Dynamics*, 36(5):723–740.

Womersley, J. R. (1955). Method for the calculation of velocity, rate of flow and viscous drag in arteries when the pressure gradient is known. *The Journal of physiology*, 127(3):553.

Yadav, P. K., Jaiswal, S., Puchakatla, J. Y., and Filippov, A. (2020). Poiseuille flow of micropolar-newtonian fluid through concentric pipes filled with porous medium. *Colloid Journal*, 82:333–341.

Zhang, X. and Wang, X. (2024). The hermite finite volume method with global conservation law. *Journal of Scientific Computing*, 98(1):17.

APPENDICES

Appendix I: Support results for Higher time frames

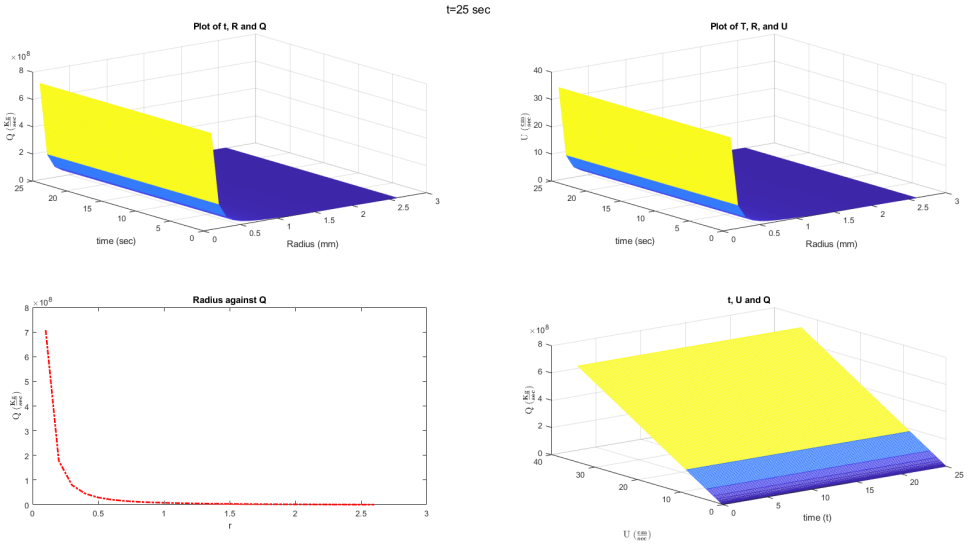

Figure 5.1: The results for simulation time of 25s sec.

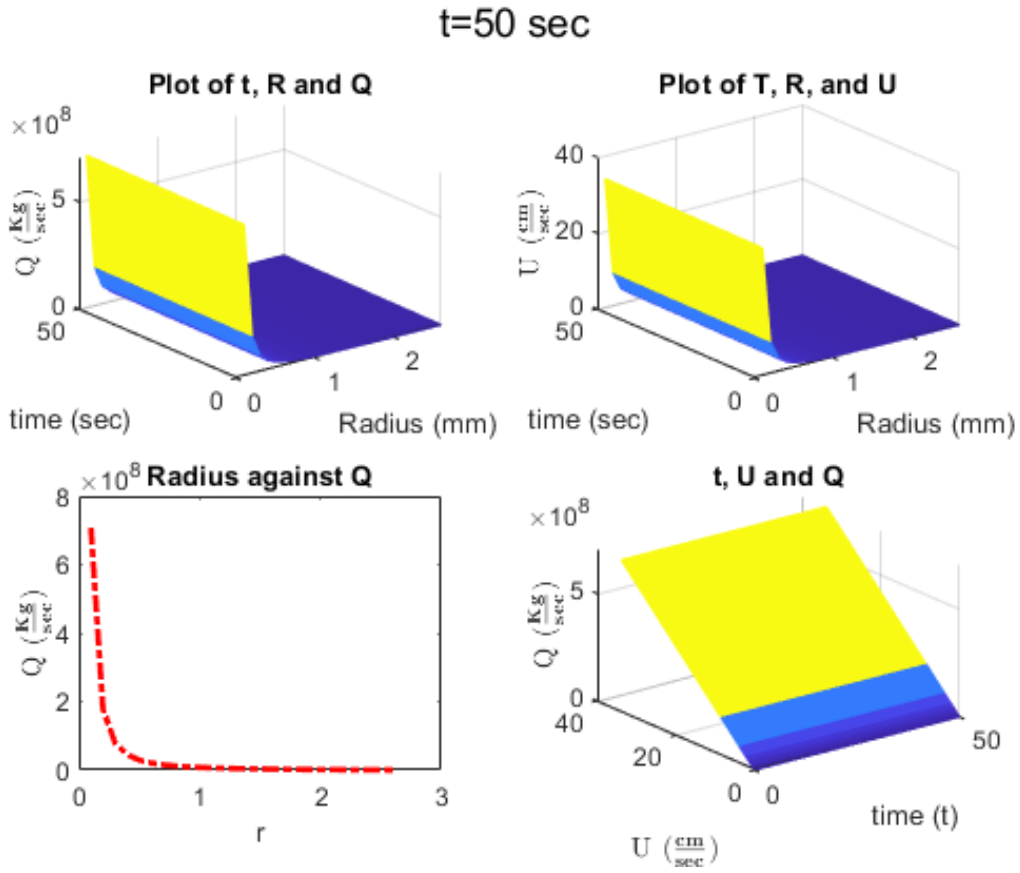

Figure 5.2: The results for simulation time of 50s sec.

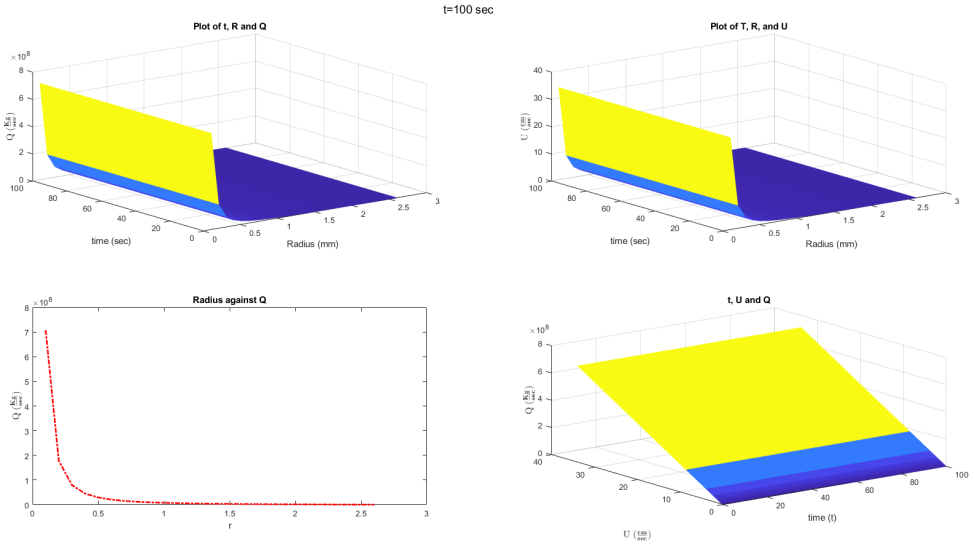

Figure 5.3: The results for simulation time of 100s sec.

Appendix II: Similarity Report

University of Eldoret

University of Eldoret

Certificate of Plagiarism Check for Thesis

Author Name	LUCY JEROP NGETICH SSCI/MAT/M/002/20
Course of Study	Type here...
Name of Guide	Type here...
Department	Type here...
Acceptable Maximum Limit	Type here...
Submitted By	lib.stoo@uoeld.ac.ke
Paper Title	MODELLING GEOMETRY INTERRUPTION, VASCULAR STRESS, AND PULSATILITY IN CAROTID ARTERY BLOOD FLOW USING POISEUILLE-BASED EQUATIONS
Similarity	10%
Paper ID	4634959
Total Pages	88
Submission Date	2025-11-06 15:30:15

Signature of Student

Signature of Guide

University of Eldoret
LIBRARIAN
06 NOV 2025
P. O. Box 1125, ELDORET - 30100
University Librarian

Head of the Department

Director of Post Graduate Studies

* This report has been generated by DrillBit Anti-Plagiarism Software